

IUE  esa



NEWSLETTER

TABLE OF CONTENTS

NO. 15

NOVEMBER 1982

Observatory Controller's Message	2
New European IUE Selection Committee	3
AIYOUUE at Apogee	4
IUE Spacecraft status	5
IUE Data reduction XVI :Orbital velocity correction	16
Photometric consequences of the microphonic avoidance technique	25
S/N characteristics LWP and LWR Cameras at High Dispersion	31
Use of the LWP Camera and its Absolute Calibration (Preliminary Report)	38
Absolute calibration of IUE High Resolution Spectra: Changes with the New Software	43
Interactive Facility for consulting the Merged Log of IUE Observations at VILSPA	52
IUE Vilspa Publications	59
Third European IUE Conference (Table of Contents)	65
Images released	76
Vilspa log of images (1 May 82 - 30 Sep 82)	85
Various Forms and Announcements Microfiche	104

IUE ESA Newsletter :

Editor: W. Wamsteker
Published by: The ESA IUE Observatory
Apartado 54065, Madrid, Spain
Telephone: +34-1-4019661
Telex: 42555 VILS E
Typing: C. Ramirez Palacios
Drawings: J. Garcia Palacios

OBSERVATORY CONTROLLER'S MESSAGE

At the time of writing this message we just have finished to collect and catalogue the proposals for the 6th round of IUE observations. There are 276 proposals, more than last year: this clearly shows that European Astronomers still like IUE!

The proposals will now be reviewed by the new European IUE allocation Committee, which has been recently appointed: names and institutions of the members of the Committee are listed on page 3 of this Newsletter.

The satellite, as you can read at page 5 and following continues to perform satisfactorily, the only critical area is the gyro system which is left without redundancy. However, a new Attitude Control Software, based on a two-gyros configuration, has already been successfully designed in case of a further failure.

Several changes in the Observatory Staff will occur during the next months: Luciana Bianchi and Patrizio Patriarchi will leave VILSPA at the end of the year to return to their home Institutions, Turin and Arcetri Observatories respectively; Chris Blades, the UK Resident Scientist, will soon move to the Space Telescope Science Institute in Baltimore. I like to thank all of them for their contribution to the IUE Project and I wish them the best success in their future activity.

More changes are expected during the next year and we will certainly look for new scientific personnel: young, active astronomers who may be available in the near future are welcome to enquire about these openings (see also page 110 of this Newsletter).

A set of microfiches containing the IUE Merged Log of the first 4 years of observations is included in the present issue. On the same subject, I like to point out the availability of an interactive computerized access to the Merged Log (see page 52) which has been recently installed at VILSPA. Our Visitors are welcome to use it and I am sure they will find it very useful for the preparation of their observations.

P. Benvenuti.

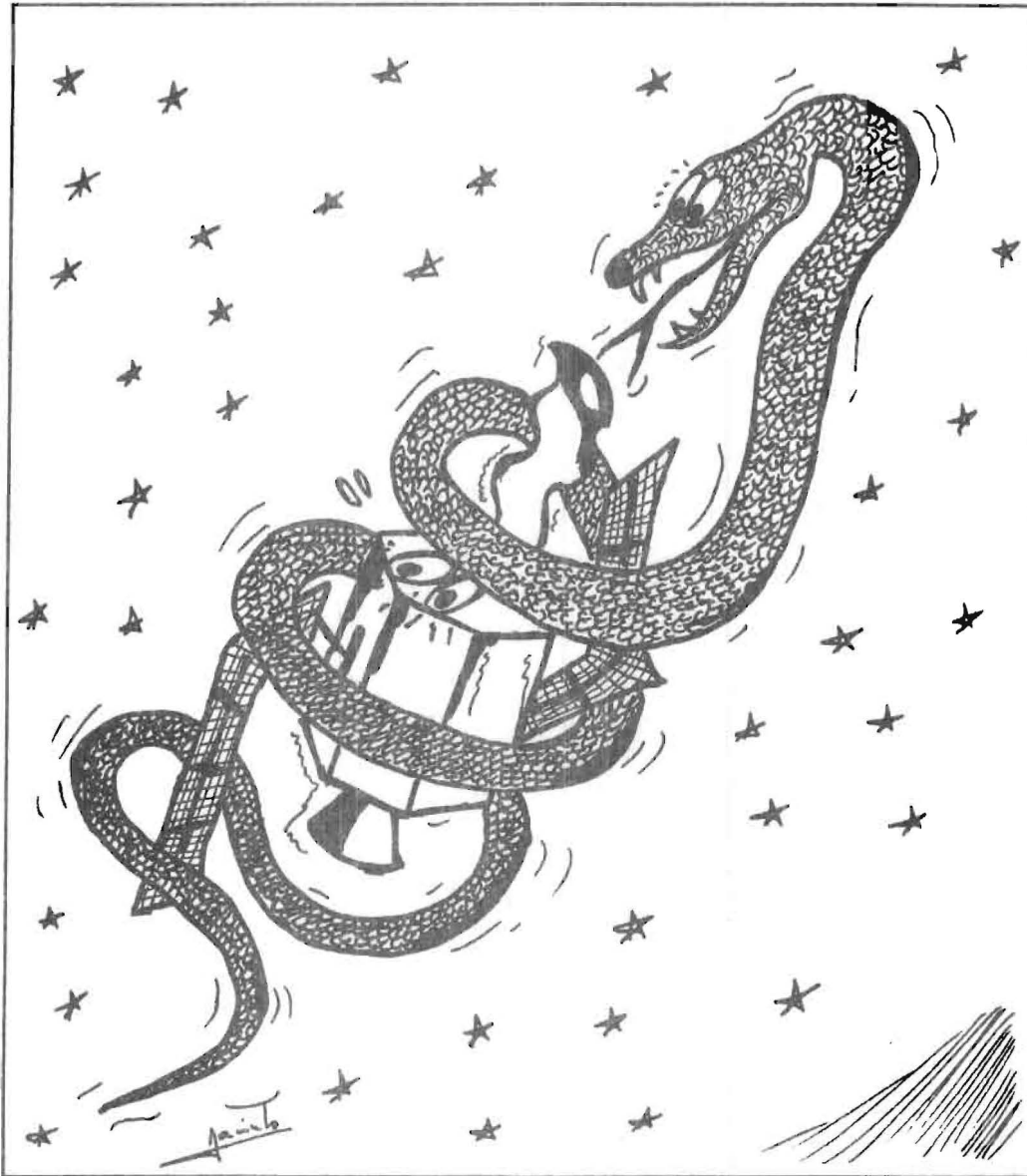
NEW EUROPEAN SELECTION COMMITTEE FOR IUE

The proposals requesting Observing time for IUE are each year evaluated by a Selection Committee. Due to the changes in the agreements between ESA and SERC made last year, a new Selection Committee had to be composed. Below we give for your information the complete list of the members of this Committee.

M. Grewing/Chairman	Astr. Institut, Tübingen
A. Willis/Vicechairman	U.C.L., London
M. Barlow	U.C.L., London
G. Bath	Dept. of Astrophys., Oxford
R. Canal	Inst. de Físicas, Barcelona
R. Carswell	Instit. of Astronomy, Cambridge
D. Clark	R.A.L., Oxon
J. Danziger	E.S.O., München
C. de Loore	Astroph. Instituut, Brussel
R. Ellis	Durham University, Durham
C. Jordan	Dept. of Theor. Phys., Oxford
R. Kudritzki	Inst. fur Theor. Physik, Kiel
H. Lamers	Space Research Lab., Utrecht
J. Lequeux	Obs. de Meudon, Meudon
A. Meadows	Dept. of Astronomy, Leicester
G. Miley	Sternwacht, Leiden
H. Nussbaumer	Atomic Phys. and Astrophys. Group, Zurich
N. Panagia	Inst. di Radio Astron., Bologna
G. Perola	Inst. Astronomico, Roma
F. Praderie	Obs. de Meudon, Meudon
J. Rahe	Remeis Sternwarte, Bamberg

SECRETARY: P. Benvenuti, VILSPA

Adventures of AIYOUEEE at apogee



This observing of Alpha Serpentis through the large aperture turns out rather different than I anticipated!!!

IUE SPACECRAFT STATUS

The spacecraft continues to support science operations normally and effectively. The solar array power output continues to decrease with life, as expected. This reduced power output limits the time one may operate at Beta angles greater than 120 or less than 20. After recharging the batteries, operation at high or low Beta may be restarted.

On July 27 Gyro-2 failed; this is the third Gyro to fail, so the spacecraft is now left without any back-up Gyro capability: the three now operating are the minimum required by the current control system. The GSFC Guidance and Control Branch is designing a control system that would use two Gyros and the Digital Fine Sun Sensor, as a back-up control system, in the event of another gyro failure. The initial control system design is nearly complete and the dynamic simulations show that this back-up control system is feasible. A high priority is placed on this work and the new control system is expected to be operational by March 1983.

Following is a complete and detailed IUE Status Report issued in the NASA IUE Newsletter Nr.18, March 1982, which we like to present to the European Community of IUE Users. The report has been updated where new figures are available or the status had changed since.

J. FAELKER.

I. SCIENTIFIC INSTRUMENT HARDWARE STATUS

A. CAMERAS (4)

- i) Long Wavelength Redundant (LWR) - standard camera.
no operational problems
- ii) Short Wavelength Prime (SWP) - standard camera.
no operational problems
- iii) Long Wavelength Prime (LWP) - available on G/O request.
read scan control frequently fails
max. 45 minutes extra overhead time for
turn on/off.
- iv) Short Wavelength Redundant (SWR) - Not available
read section grid voltages usually fail

B. SPECTROGRAPHS (2)

i) Short Wavelength

Entrance Apertures

Large Aperture (SWLA) - oval shape

Length for trailed spectra :

21.4 ± 0.4 arcsec.

Area for extended sources:

200 ± 5 sq. arcsec.

(Panek 1982a)

Small Aperture (SWSA) - probably non-circular
effective shape

area ~ 6.8 sq. arcsec (Panek 1982a)

point source throughput 0.53 ± 0.13

Orientation - variable (Schiffer 1980)

(Patriarchi 1981)

Echelle Mode - functional

Low Dispersion Mode - functional

ii) Long Wavelength

Entrance Apertures

Large Aperture (LWLA) - oval shape

Length for trailed spectra :

20.5 ± 1.0 arcsec.

area for extended sources :

203 ± 6 sq. arcsec.

(Panek 1982a)

Small Aperture (LWSA) - probably non-circular effective shape

area ~ 6.9 sq. arcsec (Panek 1982a)

point source throughput :

0.49 ± 0.15

Orientation - variable (Schiffer 1980)

(Patriarchi 1981)

Echelle Mode - functional

Low dispersion mode - functional

C. FINE ERROR SENSORS(2)

i) FES 1 - back-up system last used 1978 Feb 18
2 magnitudes less sensitive than FES 2

ii) FES 2 - standard

positional accuracy 0.27 arcsec
near center of field.

3 arcsec elsewhere

8 arcsec for $m < -0.6$ or

$14.2 < m < 16$

field size 8 arcmin radius

eff. wavelength $\sim 5200 \text{ \AA}$

visual calibration (Holm and Rice 1981)

experiences electronic confusion from

operation aperture closure mechanism and

the Sun shutter mechanism

II. SPACECRAFT (S/C) HARDWARE STATUS

A. GYROSCOPIES (6)

No. required for three-axis stabilized attitude control - 3

No. healthy - 3

Gyro-1 (failed at 1981 March 2, 19:50 GMT)

Gyro-2 (failed at 1982 July 27, 07:00 GMT)

Gyro-6 (stuck since turned off for 1979 shadow season)

No. failed - 3

S/C drift rates - 3 to 20 arcsec/hour (in pitch & yaw)

usually largest shortly after slewing

Maneuver accuracy since 1981 Nov 21

error/length $\sim 4 \times 10^{-4}$ (Panek and Baroffio 1982)

B. REACTION WHEELS(4)

No. required for slewing - 3

No. in use - 3 (pitch, yaw, and roll)

Backup (skewed wheel) never used in orbit

C. HYDRAZINE SYSTEM

Required for reaction wheel maintenance, orbit change maneuvers, and emergency sun acquisitions
 ~ 22 kg available
 usage rate ~ 0.5 kg/year

D. SOLAR ARRAYS AS OF 1982 MAY

75% of capacity at launch (Fragola & Espejo 1982)
 Power positive zone - depends upon activity level
 Beta angles 120 to 20 with 1 camera reading
 and 1 camera exposing

E. BATTERIES(2)

Max. depth of discharge during September 1982 shadow season
 Battery #1 61.34%
 Battery #2 61.18%

F. ON-BOARD COMPUTER(2)

i) OBC 1

Temperature limit 55.8 C
 Last crash 1982 Feb 21 (1.3 hours lost)
 Software systems
 8K - standard
 4K - new crash resistant system
 capable of supporting science operations
 - bug in attitude control logic

ii) OBC 2

backup system
 never used in orbit

III. IMAGE PROCESSING SYSTEM STATUS

(Alderman, Turnrose, and Northover 1981)

The current system has evolved through a series of modifications. The following list is my interpretation of the most significant modifications and their implementation dates (VILSPA date in parenthesis).

Averaged Intensity Transfer Function 1978 May 22 (78 June 14)

Improved λ calibration Line Library

Low dispersion	1978 Sept 21 (79 Feb 01)
High dispersion	1979 Nov 23 (81 Mar 10)
Correct SWP ITF error	1979 Jul 07 (79 Aug 07)
Mean dispersion constants:	
Low dispersion	1979 Oct 30 (81 Mar 10)
High dispersion	1980 Jul 18 (81 Mar 10)
Improved λ calibration Line Library	
"New" Low dispersion software	
Parameterized low dispersion constants	1980 Nov 4 (81 Mar 10)
Parameterized high dispersion constants	1981 May 19 (82 Mar 11)
"New" High dispersion software	1981 Nov 10 (82 Mar 11)

IV. INSTRUMENTAL PERFORMANCE

A. NOISE

- i) Readout noise ~ 10 DN/pixel
- ii) Periodic noise (microphonics)
 - SWP - covers entire image
amplitude generally 1-3 DN
amplitude may be increased to 10-40 DN
by mechanical activity in S/C, incl.
roll slews
frequency ~ 200 Hz (Northover 1979)
 - LWR - affects a few lines in $\sim 85\%$ of images
amplitude up to 110 DN
amplitude decays $\sim 25\%$ image line (Panek 1981)
frequency ~ 300 HZ (Panek 1981)
occurrence associated with heating of
read section of camera
occurrence modified by delaying
read (Holm and Panek 1982)
 - LWP - occurrence associated with Roll slews
amplitude up to 7 DN.
affects only the lines when a roll slew is
in progress (Faelker 1982)
- iii) Bright spots
 - radioactive disintegrations in phosphor ~ 30 spots/hr
(Coleman et al. 1977)
 - permanent blemishes
 - most pronounced pseudo-emission feature
 ~ 2190 A low dispersion, large aperture
others (Ponz 1980)

iv) Typical signal/noise ratio

for well exposed point source spectra

SWP 10-30 old software (Cassatella et al. 1980)

7-27 new software

LWR 12-21 old software (Settle et al. 1981)

8-15 new software (Barylak 1982)

LWP 9-25 old software (Settle et al. 1981)

6-18 new software (Barylak, 1982)

v) S/N properties of averaged spectra

(Clarke 1981a)

(West and Shuttleworth 1981)

B. BACKGROUND

i) Phosphorescence fogging

During low-radiation shifts

LWR & SWP 6-10 DN/hour/pixel

LWP 4-7 DN/hour/pixel (Ake 1982)

Fogging rate depends on no. and type of PREPS before exposure

Overexposures cause "ghost" spectrum fogging phosphorescence decay rate

~ $t^{-0.8}$ up to several hours (Coleman 1978)

unknown after long time intervals

ii) Radiation fogging

caused by Cerenkov radiation from electrons in the van Allen belts (Coleman et al. 1977)

may be severe near perigee (US shift 2)

recent experience 22% low fogging shifts

15% high fogging shifts

C. PHOTOMETRIC PROPERTIES

i) Upper limits to ITFs (Turnrose 1980)

ii) Linearity errors in processed spectra

SWP -10 to -20 percent for Net DN < 20

+10 to +15 percent for ave. DN > 220 @ 1300 Å

(Holm 1981b)

LWR +10 to +20 percent for Net DN < 40

LWP -5 to -10 percent for Net DN < 50

(Settle et al. 1981)

possibly better with ITF 1

D. ABSOLUTE CALIBRATION

- i) Low dispersion SWP and LWR (Holm et al. 1982)
- ii) High dispersion SWP and LWR (Cassatella et al. 1981)
For new software (Cassatella et al. 1982)
- iib) Low dispersion LWP (Blades & Cassatella 1982)
- iii) High dispersion software
LWP - not yet available
- iv) Accuracy of standards
 $\pm 10\%$ 1300A - 3400 A
- v) Echelle ripple correction (Ake 1981)

E. SENSITIVITY VARIATION

- i) Temperature dependence (Schiffer 1982a)
SWP -0.5% / C of head amplifier temperature (THDA)
LWR -1.1% / C of THDA
LWP unknown
- ii) Repeatability (1σ after temperature correction)
(Schiffer 1982a)
SWP 2% in 150 A bins
LWR 2.5% in 300 A bins
LWP unknown
- iii) Temporal dependence (Schiffer 1982a)
SWP -6.3% /year @ 1850 A before 1979.3
 $<0.3\%$ /year since 1979.3
LWR $<1\%$ /year until mid 1980
 -4.5% /year @ 2400 A and 2600 A since mid 1980
LWP unknown

F. WAVELENGTH RESOLUTION

- i) Short wavelength echelle mode
small aperture FWHM 0.085 A @ 1150 A
(Boggess et al. 1978)
0.19 A @ 2100 A
(Boggess et al. 1978)
large/small 1.01 (Penston 1979)

- ii) Short wavelength low dispersion mode
 large aperture FWHM 6.1 Å
 (Cassatella & Penston 1978)
 large/small 0.99±0.7
 (Ponz & Cassatella 1981)
- iii) Long wavelength echelle mode
 small aperture FWHM 0.20 Å
 (Boggess et al. 1978)
 large/small 1.09
 (Penston 1979)
- iv) Long wavelength low dispersion mode
 large aperture FWHM 9.2 Å
 (Cassatella & Penston 1978)
 large/small 1.17±0.15
 (Ponz & Cassatella 1981)

G. WAVELENGTH ACCURACY

- i) Internal consistency of wavelength calibration determinations (Thompson et al. 1981)

SWP 2.0 km/sec
 LWR 2.7 km/sec
 LWP unknown

- ii) Possible systematic errors

SWP unknown now
 early data (Leckrone 1980)
 LWR ~10 km/sec
 LWP unknown

H. MISCELLANEOUS

- i) Grating scattered light
 (Clarke 1981b)
 Stickland 1980)
- ii) Halation: Backscattering of Electrons from the phosphor decay length ~32+3 pixels (Coleman 1978)
- iii) Scattered Light in the Telescope
 $F_{\text{scat}} \sim d^{-2.5} F_*$ (Schiffer 1982b)
 where d is in arcsec ($5 \langle d \rangle 40$)

- iv) Plate scale
1.51±0.04 arcsec/pixel
- v) Residual geometric errors in geometrically corrected image
±0.4 arcsec = ±0.2 pixels (Panek et al. 1982)
- vi) Exposure timing (Schiffer 1980b, Heck 1981)
command units 0.4096 seconds
effective response delay 0.12 seconds LWR & SWP
unknown LWP
- vii) Longest Exposure to Date
SWP 15293 1273 minutes

REFERENCES

- Ake, T.B. 1981, NASA IUE Newsletter, No. 15, p. 60
- Ake, T.B. 1982, IUE Internal memo
- Alderman, D.F., Turnrose, B.E., and Northover, K.J.E. 1981, NASA IUE Newsletter, No. 15, p. 77; ESA IUE Newsletter, No 11, p 75
- Blades, J.C., and Cassatella, A., 1982, ESA IUE Newsletter No 15, p 38
- Boggess, A., et al. 1978, Nature, 275, 377
- Bohlin, R.C., and Holm, A.V. 1980, NASA IUE Newsletter, No. 10, p. 37, ESA IUE Newsletter, No. 11, p. 18
- Cassatella, A., and Penston, M. 1978, ESA IUE Internal memo MP/cr-116
- Cassatella, A., Holm, A., Ponz, D., Schiffer, F.H. 1980, NASA IUE Newsletter, No. 8, 1
- Cassatella, A., Ponz, D., and Selvelli, P.L. 1981, NASA IUE Newsletter, No. 14, p. 170 ; ESA IUE Newsletter No. 10, p 31
- Cassatella, A., Ponz, D., Selvelli, P.L., 1982, ESA IUE Newsletter, No 15, p 43
- Clarke, J.T. 1981a, NASA IUE Newsletter, No. 14, 149
- Clarke, J.T. 1981b, NASA IUE Newsletter, No. 14, 143
- Coleman, C.I. 1978, paper presented at the Seventh Symposium on Photoelectric Image Devices at Imperial College, September 1978
- Coleman, C.I., Golton, E., Gondhalekar, P., Hall, J., Oliver, M., Sandford, M., Snijders, T., and Stewart, B., B. 1977, IUE Technical Note No. 31
- Crabb, W. 1981, Report to the Three-Agencies
- Faelker, J. 1982, Memorandum "Periodic Noise (Microphonics) on the LWP Camera"
- Fragola, J., and Espejo, P. 1982, Bendix report
- Heck, A. 1981, ESA IUE Newsletter, No. 13, p. 40
- Holm, A.V., 1981a, NASA IUE Newsletter, No. 15, p. 95
- Holm, A.V., 1981b, NASA IUE Newsletter, No. 15, p. 70
- Holm, A.V., and Rice, G. 1981, NASA IUE Newsletter, No. 15, p. 74, ESA IUE Newsletter, 11, 15
- Holm, A.V. and Panek, R.J. 1982, NASA IUE Newsletter, No. 18
- Holm, A.V., Bohlin, R.C., Cassatella, A., Ponz, D., Schiffer III, F.H. 1982, Astron. Astrophys. 107, 205
- Leckrone, D.S. 1980, NASA IUE Newsletter, No. 10, p. 25
- Northover, K.J.E. 1979, ESA IUE Newsletter, No 11, p 27
- Panek, R.J. 1981, Report to the Three-Agencies b Panek, R.J., 1982a, NASA IUE Newsletter, No. 18, ESA IUE Newsletter, No. 15, p.
- Panek, R.J., and Baroffio, B. 1982, IUE Internal memo
- Panek, R.J., Holm, A.V., and Schiffer, F.H., III 1982, in "Instrumentation in Astronomy IV. SPIE Proceedings Vol. 331"
- Patriarchi, P., 1981, ESA IUE Newsletter, No 10, p 7
- Penston, M. 1979, Report to the Three Agencies
- Ponz, D. 1980, ESA IUE Newsletter, No. 8, p. 12
- Ponz, D., Cassatella, A.C., 1981, Report to Three Agencies
- Schiffer, F.H. 1980a, NASA IUE Newsletter, No 9, p 32
- Schiffer, F.H. 1980b, NASA IUE Newsletter, No. 11, p. 33

Schiffer, F.H. 1982a, NASA IUE Newsletter, No. 18
Schiffer, F.H. 1982b, IUE Internal memo
Settle, J., Shuttleworth, T., and Sandford, M.C.W. 1981, NASA IUE
Newsletter, No. 15, p. 97
Thompson, R.W., Turnrose, B.E., and Bohlin, R.C. 1981, NASA IUE
Newsletter, No. 15, p. 8
Turnrose, B.E. 1980, NASA IUE Newsletter, No. 9, p. 13
West, K., and Shuttleworth, T. 1981, ESA IUE Newsletter, No. 12,
p. 27

IUE DATA REDUCTION

XVI. Orbital Velocity Corrections

INTRODUCTION

The resolving power ($R = \lambda/\text{FWHM}$) of the IUE spectrographs varies from 1.0×10^4 to 1.5×10^4 over the entire wavelength range covered (Boggess, et al., 1978). Therefore the IUE velocity resolution varies from 20 km s^{-1} to 30 km s^{-1} . If it is assumed that the centroid of a line can be determined to approximately 10% of its FWHM, then a measured radial velocity should be accurate to about 2 km s^{-1} (best case). The orbital velocity of the Earth about the Sun ($\sim 30 \text{ km s}^{-1}$) and the velocity of the spacecraft about the Earth ($\sim 4 \text{ km s}^{-1}$ at perigee) are both larger than the best possible velocity determinations and their effect should be removed from the data.

Two subprograms, VELSUN and VELSAT, have been written for IUESIPS, the International Ultraviolet Explorer Spectral Image Processing System, to calculate orbital velocities. VELSUN determines the velocity vector of the Earth at a given time using the orbital elements of the Earth and the time derivatives of these elements (A. E., 1980). VELSAT determines the velocity vector of the spacecraft about the Earth at a given time using all the orbital elements of the spacecraft for Nov. 22, 1979, except for the period, which is set to exactly one sidereal day. Since the orbit of the spacecraft is periodically adjusted to maintain a sidereal period and, moreover, an approximately fixed ground path, it is not necessary to update the orbital elements used by the program. This program is accurate to $\pm 0.25 \text{ km s}^{-1}$ over the entire life of the spacecraft (launch to present), and VELSUN is accurate to better than 0.01 km s . Both of these subprograms will be added to IUESIPS in the near future.

The following sets of equations giving the rectangular coordinates of a body in its orbit as a function of the orbital elements were adopted (A. D. Dubyago, 1961):

$$\left. \begin{aligned} x &= r(\cos u \cos \Omega - \sin u \cos i \sin \Omega), \\ y &= r(\cos u \sin \Omega + \sin u \cos i \cos \Omega), \\ z &= r \sin u \sin i. \end{aligned} \right\} \text{and} \quad (1)$$

$$\mu = \frac{k\sqrt{1+m}}{a^{3/2}} = \frac{2\pi}{P} = n$$

$$E - e \sin E = M_0 + \mu (t - t_0) = M, \quad (2)$$

$$\left. \begin{aligned} r \sin v &= a \sqrt{1 - e^2} \sin E, \\ r \cos v &= a(\cos E - e), \end{aligned} \right\} \quad (3)$$

$$u = v + \omega$$

The first three equations (set 1) give the position of the orbiting body in a rectangular coordinate system. The +X axis is toward the Vernal Equinox and the +Z axis is in the direction from the origin toward the celestial pole or the Ecliptic pole (depending on the system of the orbital elements). The coordinate system is righthanded.

The orbital elements, constants and various intermediate quantities used in the equations are listed below,

The orbital elements are:

a = semi major axis (kilometers)

i = inclination of orbit to ecliptic or equator (Radians)

T = time of pericenter passage (Julian Date)

e = eccentricity

ω = the argument of pericenter (the angle between the ascending node and pericenter measured along the orbit) (Radians)

Equinox and the line of nodes - measured along the ecliptic or
equator from the Vernal Equinox to the ascending node) (Radians)

and P = the period in years.

Other quantities used in the equations:

m = mass of orbiting body

$\mu = n =$ the mean angular motion

k = gaussian constant = $\frac{2\pi a^{3/2}}{P\sqrt{1+m}}$

$\pi = 3.14159265$

E = eccentric anomaly

M = mean anomaly

$M_0 =$ mean anomaly at time t_0

$t_0 = T =$ time when $M_0 = 0$

v = true anomaly (the angle between pericenter and the position of the
body - measured along the orbit)

r = distance from primary to the orbiting body

u = longitude of pericenter (sometimes designated θ) - the sum of the
angles v and ω

The equations in set (1) were differentiated with respect to time to obtain the
following set of equations defining the velocity vector of the body:

$$\left. \begin{aligned} V_x &= (\mu/V_3) \left[aV_2(C_4C_3C_7 - C_5C_8) - C_1V_1(C_5C_7 + C_4C_3C_8) \right] \\ V_y &= (\mu/V_3) \left[C_1V_1(C_4C_5C_8 - C_3C_7) - aV_2(C_4C_5C_7 + C_3C_8) \right] \\ V_z &= (\mu C_2/V_3) (C_1C_8V_1 - aC_7V_2) \end{aligned} \right\} \quad (4)$$

where

$$C_1 = a(1-e^2)^{1/2}$$

$$C_2 = \sin(i)$$

$$C_3 = \sin(\Omega)$$

$$C_4 = \cos(\Omega)$$

$$C_5 = \cos(\omega)$$

$$C_7 = \sin(\omega)$$

$$C_8 = \cos(\omega)$$

$$V_1 = \cos(E)$$

$$V_2 = \sin(E)$$

$$V_3 = [1 - e \cos(E)]$$

The program VELSAT uses this set of equations in this form with orbital elements referred to the equatorial system. VELSUN uses the orbital elements of the Earth referred to the ecliptic system which leads to a simplified set of equations since in this case $i=0$ and Ω can be given an arbitrary value (set $\Omega = 0$). The following set of equations, derived from set (4) give the rectangular velocity components of the Earth in the ecliptic system:

$$\left. \begin{aligned} V'_x &= -(\mu/V_3) (aC_8V_2 + C_1C_7V_1) \\ V'_y &= (\mu/V_3) (C_1C_8V_1 - aC_7V_2) \\ V'_z &= 0.0 \end{aligned} \right\} (5)$$

To obtain the velocities in the equatorial system from these the following relations are used:

$$\begin{aligned} V_x &= V'_x \cos(\epsilon) \\ V_y &= V'_y \cos(\epsilon) \\ V_z &= V'_z \sin(\epsilon), \end{aligned}$$

where $\epsilon =$ the obliquity (about 23°).

Since these equations involve the eccentric anomaly, E , in addition to the orbital elements it was necessary to solve equation (2) (Keplers Equation) for E where the known values are e , M_0 , μ , t_0 and t . In order to solve this equation the following series approximation (W. M. Smart, 1965) was used:

$$E = M + \left(e - \frac{e^3}{8}\right) \sin(M) + \frac{1}{2}e^2 \sin(2M) + \frac{3}{8}e^3 \sin(3M)$$

The eccentricity of the IUE's orbit is 0.23 which causes an error in E with this approximation of about 0.1 radian. The Earth's orbital excentricity is so small that the approximation causes no appreciable error.

FORTRAN LISTINGS

Listings of the two FORTRAN subroutines, VELSUN and VELSAT are given in Appendix A. Program documentation is in the form of in-line comment statements. Table 1 presents a set of sample input and output for each of the subroutines.

C. Harvel

References:

- A. E. (1980). The American Ephemeris and Nautical Almanac (U. S. Government Printing Office, Washington), page 544.
- Bogges, A. et al. (1978). In-Flight Performance of the IUE, Nature, 275, 7.
- A. D. Dubyago (1961). The Determination of Orbits (The Macmillan Company, New York), p. 49
- Smart W. M. (1965). Text -Book on Spherical Astronomy (Cambridge University Press, Cambridge), Chap. 5.

APPENDIX A

SUBROUTINE VELSUN(TIME,VX,VY,VZ,IERROR)
 IMPLICIT REAL*8(A-H,O-Z)

REAL*8 INC,NODE,MØ

ORIGINAL PROGRAM WRITTEN BY HOWARD L. COHEN AND ARTHUR
 YOUNG INDIANA UNIVERSITY ASTRONOMY DEPT.(PGM NAME
 WAS 'ORBVAL'). CIRCA 1965

PROGRAM REWRITTEN BY C. HARVEL 1/24/8Ø
 COMPUTER SCIENCE CORPORATION, DEPT. OF ASTRONOMY

PROGRAM MODIFIED BY DAK 1/2Ø/78
 GIVEN THE TIME THIS PROGRAM COMPUTES THE THREE
 COMPONENTS OF THE EARTHS RADIAL VELOCITY,VX,VY,VZ(RIGHT
 HANDED COORDINATE SYSTEM--- X POSITIVE TOWARD THE VERNAL
 EQUINOX AND Z POSITIVE TOWARD THE NORTH.
 VX,VY,VZ IN KM/SEC. TIME-JD-24ØØØØØ.ØØØ(ELEMENTS ARE IN
 ECLIPTIC SYSTEM.) THE ERROR CODE IERROR=Ø IF THERE ARE
 NO ERRORS AND 1 IF THE TIME GIVEN IS OUTSIDE THE
 RANGE JDI TO JDF.

REAL*8 MA,MU,JDI,JDF,E(3),OB(3),OM(3),M(3),SP(2)

DATA PIE/3.1415926535898DØ/
 DATA JDI,JDF /1.5Ø2D4, 5.15445D4/
 DATA E /Ø.Ø16751Ø4DØ,1.1444D-9, 9.4D-17/
 DATA OB /Ø.4Ø9319747DØ, 6.2179Ø99D-9, 2.146755D-17/
 DATA OM /1.7666368Ø7DØ, 8.21499D-7, 5.916666D-15/
 DATA M /6.25658378DØ, 1.72Ø196977D-2, 1.9547668D-15/
 DATA SP /365.25636Ø42DØ, 1.1D-7/
 DATA A /1.496D8/
 IERROR=Ø

THE DATA ABOVE ARE TAKEN FROM THE AMERICAN EPHEMERIS
 AND NAUTICAL ALMANAC(198Ø) PAGE 544(THE EXPLANATION
 SECTION). JDI-THE EPOCH OF THE DATA(JULIAN DATE OF
 EPOCH MINUS 24ØØØØØ), JDF- FINAL JULIAN DATE BEYOND
 WHICH THESE DATA ARE INVALID, E-THE ECCENTRICITY(2ND
 AND 3RD ENTRIES IN THESE ARRAYS ARE THE 1ST AND 2ND TIME
 DERIVATIVES). OB-THE OBLIQUITY OF THE ECLIPTIC(IN RADIANS),
 OM-THE LONGITUDE OF PERIHELION(RADIANS), M-THE MEAN ANOMALY
 (RADIANS), SP-THE SIDERIAL PERIOD(DAYS) AND A-THE SEMIMAJOR
 AXIS(KILOMETERS).

IF(TIME.LT.JDI.OR.TIME.GT.JDF) GO TO 5
 GO TO 1Ø
 IERROR=1
 RETURN
 STOP

1Ø CALCULATE ELAPSED TIME SINCE JD 2415Ø2Ø.Ø
 D= TIME-JDI
 D2= D*D
 CALCULATE THE ECCENTRICITY
 ECC= E(1) - E(2) * D - E(3) * D2
 CALCULATE THE OBLIQUITY OF THE ECLIPTIC
 OBL= OB(1) - OB(2) * D - OB(3) * D2
 CALCULATE THE LONGITUDE OF PERIHELION
 OMEGA= OM(1) + OM(2) * D +OM(3) * D2
 CALCULATE THE MEAN ANOMALY

APPENDIX A

```

C      MA= M(1) + M(2) * D - M(3) * D2
C      CALCULATE THE ECCENTRIC ANOMALY
C      EA=MA+(ECC-(ECC**3)/B.DB)*DSIN(MA)+(B.5*ECC*ECC*
1      DSIN(2.*MA)+(B.375*(ECC**3)*DSIN(3.*MA)))
C      CALCULATE THE EARTHS SIDERIAL PERIOD
C      P=( SP(1) + SP(2) * D ) * B.64DB4
C      CALCULATE THE MEAN MOTION
C      MU=(2.DB*PIE)/P
C
C      C1=A*(1.DB-ECC**2)**B.5
C      C2 THROUGH C6 NOT USED FOR EARTH ORBIT
C      C7=DSIN(OMEGA)
C      C8=DCOS(OMEGA)
C      V1=DCOS(EA)
C      V2=DSIN(EA)
C      V3=(1.DB-ECC*V1)
C
C      VXECL= -(MU/V3)*(A*C8*V2+C1*C7*V1)
C      VYECL= (MU/V3)*(C1*C8*V1-A*C7*V2)
C      VZECL = B.DB
C
C      VXECL,VYECL AND VZECL ARE THE VELOCITIES IN THE
C      ECLIPTIC SYSTEM.
C
C      VX= VXECL
C      YY= VYECL*DCOS(OBL)
C      VZ= VYECL*DSIN(OBL)
C
C      RETURN
C      END

```

THE DATA ABOVE ARE TAKEN FROM THE AMERICAN LUNAR EPHEMERIS AND PERTAIN TO THE PERIOD FROM 1950 TO 1960. THE EVALUATION SECTION 1.1 OF THE DATA SHEET DATE OF WHICH THIS DATA WAS DERIVED IS THE EARTH'S ORBITAL PERIOD AND THE DATA ARE IN THESE ARRAYS ARE THE 1ST AND 2ND TIME DERIVATIVES OF THE ORBITAL PERIOD. THE DATA ABOVE ARE TAKEN FROM THE AMERICAN LUNAR EPHEMERIS AND PERTAIN TO THE PERIOD FROM 1950 TO 1960. THE EVALUATION SECTION 1.1 OF THE DATA SHEET DATE OF WHICH THIS DATA WAS DERIVED IS THE EARTH'S ORBITAL PERIOD AND THE DATA ARE IN THESE ARRAYS ARE THE 1ST AND 2ND TIME DERIVATIVES OF THE ORBITAL PERIOD.

THE DATA ABOVE ARE TAKEN FROM THE AMERICAN LUNAR EPHEMERIS AND PERTAIN TO THE PERIOD FROM 1950 TO 1960. THE EVALUATION SECTION 1.1 OF THE DATA SHEET DATE OF WHICH THIS DATA WAS DERIVED IS THE EARTH'S ORBITAL PERIOD AND THE DATA ARE IN THESE ARRAYS ARE THE 1ST AND 2ND TIME DERIVATIVES OF THE ORBITAL PERIOD.

SUBROUTINE VELSAT(TIME,VX,VY,VZ,IERROR)
IMPLICIT REAL*8 (A-H,O-Z)

REAL*8 INC,NODE,MA,MU,MØ,JDI,JDF

PROGRAM WRITTEN BY C. HARVEL 1/24/88
COMPUTER SCIENCES CORPORATION,DEPT. OF ASTRONOMY

GIVEN THE TIME (JULIAN DATE) THIS PROGRAM COMPUTES
THE THREE COMPONENTS OF THE SATELLITES (IUE)
RADIAL VELOCITY---VX,VY,VZ. COORDINATE SYSTEM IS
RIGHT HANDED WITH X POSITIVE TOWARD THE VERNAL
EQUINOX, AND Z POSITIVE TOWARD THE NORTH.
VX,VY,VZ ARE IN KM/SEC, TIME=JULIAN-DATE MINUS
2400000.0. ALL ELEMENTS ARE REFERED TO THE EARTH'S
EQUATOR(NOT THE ECLIPTIC). THE ERROR CODE IERROR=Ø
IF THERE ARE NO ERRORS AND 1 IF THE TIME IS NOT
IN THE RANGE JDI TO JDF.

TIME=JD-2400000.000
VX,VY,VZ= VELOCITIES IN KM/SEC

DATA A,INC,T,ECC,OMEGA,NODE,P,MØ,PIE/4.21632DØ4,
1 8.4934541DØ,44199.5DØ,Ø.2359693DØ,4.7283238DØ,3.385275DØ,
2 8.61642DØ4,4.3Ø32838Ø4DØ,3.14159265359DØ/
DATA JDI,JDF / 43199.DØ, 462ØØ.DØ /

THE DATA ABOVE ARE TAKEN FROM THE IUE PREDICTED
SATELLITE MAP TABLE (NASA, GODDARD--NOV. 22, 1979).
ALL DATA ARE FOR THE EPOCH JD2444199.5 (NOV. 22,1979).
A=SEMI MAJOR AXIS(KM), INC=INCLINATION TO EQUATOR(RADIANS),
T=EPOCH, ECC=ECCENTRICITY, OMEGA=LONGITUDE OF PERIGEE
(RADIANS), NODE=RIGHT ASCENSION OF THE ASCENDING NODE
(RADIANS), P=SIDERIAL PREIOD, MØ=MEAN ANOMALY AT EPOCH.

IERROR=Ø

IF(TIME.LT.JDI.OR.TIME.GT.JDF) GO TO 5
GO TO 1Ø

5 IERROR=1
RETURN
STOP

1Ø MU=(2.*PIE)/P
MA=MU*(TIME-T)*8.64DØ4+MØ
EA=MA+(ECC-(ECC**3)/8.)*DSIN(MA)+(Ø.5*ECC*ECC*
1 DSIN(2.*MA)+(Ø.375*(ECC**3)*DSIN(3.*MA)))

C1=A*(1.-ECC**2)**Ø.5
C2=DSIN(INC)
C3=DSIN(NODE)
C4=DCOS(INC)
C5=DCOS(NODE)
C6= NOT USED
C7=DSIN(OMEGA)
C8=DCOS(OMEGA)

V1=DCOS(EA)
 V2=DSIN(EA)
 V3=(1.-ECC*V1)

VX=(MU/V3)*(A*(C4*C3*C7-C5*C8)*V2-C1*(C5*C7+C4*C3*C8)*V1)
 VY=(MU/V3)*(C1*(C4*C5*C8-C3*C7)*V1-A*(C4*C5*C7+C3*C8)*V2)
 VZ=(MU*C2/V3)*(C1*C8*V1-A*C7*V2)

RETURN
 END

TABLE 1
 Sample Input/Output Values for Programs

Program	Input Time JD-2400000	Vx (km/sec)	Vy (km/sec)	Vz (km/sec)
VELSUN	43251.0D0	0.13207D+02	-0.24371D+02	-0.10568D+02
VELSAT	43251.0D0	0.18857D+01	0.15146D+01	-0.54586D+00

PHOTOMETRIC CONSEQUENCES OF THE MICROPHONIC AVOIDANCE TECHNIQUE

The resident astronomers have completed the minimal testing required to detect any serious photometric errors which might be introduced by the LWR ping avoidance technique (in which the heater warmup time before the read is extended by 4 minutes). The testing consisted of sequences of alternating normal and ping avoidance reads. No significant differences could be found in the net extracted spectra of well exposed images. Flat field images did indicate that the gross flux number is marginally higher in the ping avoidance reads i.e. the target is read out more heavily after the extended heater warmup. Much of this would cancel out in the background subtraction for the net spectra. No careful study of linearity has been made. However, the natural variations along the spectra due to spectral sensitivity and grating blaze, and the high order echelle spectra where the interorder background is high, provide a zero-order verification of linearity. Only a few strong absorption lines have been studied.

We therefore believe that there will be many instances in which the observer can gain the benefits of ping avoidance without significant photometric error. Our test results are described below in some detail since the comparisons of the spectra are of general interest as an illustration of the repeatability and signal/noise of LWR spectra.

A) Studies of flat field images

Based on 3 sequences totalling 7 images in all, we find that the ping avoidance nulls have 97 ± 64 flux numbers (FN) more than the null read normally. Based on only one series of 3 tungsten flood lamp exposures, we found the intermediate level exposures to be about 60 FN brighter when read with the ping avoidance technique. The available data is consistent with the change in FN being insensitive to exposure level.

B) Studies of low dispersion, trailed spectra

A sequence of 4 exposures, each a 31.2 s trail on HD60753, was obtained as follows:

LWR10930	test read	
LWR10931	normal read	here, 'test read' refers to the ping
LWR10932	test read	avoidance read
LWR10933	normal read	

To study differences between the derived net fluxes, we studied ratios of the net flux spectra. The ratio of two normal reads illustrates the expected level of repeatability and signal/noise. Several typical examples are shown on the next page.

C) Studies of low dispersion, point spectra

A sequence of three 24 s exposures of BD+75°325 was obtained, sandwiching a test read between two normal reads. Again, the test spectrum agreed within the expected limits for normally read spectra.

A Technique for Avoiding Microphonics on the LWR Camera

It is possible to reduce the probability of contamination of LWR images by microphonic noise "pings" by extending by 4 minutes the warmup of the cathode heater prior to the read. As seen in the table below, the probability of a ping is reduced from about 80% to about 15%. Furthermore, the pings which do occur tend to fall much higher in the image, averaging 1/7 of the way down from the top. In contrast, the pings in normally read images tend to fall about 1/3 of the way up from the bottom.

The effects of the extended heater warmup on other aspects of the spectral images are yet to be fully explored. However, some testing for photometric changes is described in the attached report. While a slight change in flat field images is detectable, no significant effects were discerned in the net spectra extracted from well exposed images.

At the present, the observatory staff recommends that this technique be used only when as warranted by the benefits of ping avoidance. Observers are urged to evaluate the test results in the context of their particular program. Note that the read will require an extra 4 minutes.

The read procedures have been modified so that the telescope operators can perform the ping avoidance reads routinely when requested on the observing form.

LWR Ping Statistical Data

type of read	No. of images	% with a ping	* y	y range	period
4 ^m extra warmup	114	15	790	615-895	Spring '81
normal warmup	312	85	435	154-727	Spring '81

* y is line number; y=895 at the top and 127 at the bottom of the image.

For the low dispersion spectra,

$$\text{wavelength (A)} = \begin{cases} 5184 - 4.662 * y & \text{large aperture} \\ 5281 - 4.662 * y & \text{small aperture} \end{cases}$$

For the high dispersion spectra,

Mg II λ 2795 is at $y \approx 320$

Mg II λ 2803 is at $y \approx 230$ in order 83 and at $y \approx 650$ in order 82.

D) Studies of high dispersion spectra

Four 26 s exposures of Lambda Leporis, B1 IV, were obtained in the order:

LWR11196 normal read
 LWR11197 test read
 LWR11198 normal read
 LWR11199 test read

Ratios between the test reads and the normal reads were formed for the extracted spectra for orders 81, 82, 83 and 100. Several typical results are shown on the next page.

Equivalent widths, residual intensities, and radial velocities were checked for the MgII lines and for the sharp interstellar FeII line at 2599 Å in order 89. The values for LWR9758 are also given to indicate the dispersion among normally read images widely separated in time.

Image	type	2795 Å (order 83)			2803 Å (order 82)			both	
		EW (Å)	% residual	V_r	EW (Å)	% residual	V_r	V_r	
LWR11196	N	0.543±.002	-0.9±0.9	12.1	0.451±.003	8.0±0.0	-10.1	10.4	
LWR11197	T	0.500 .002	-0.8 0.8	15.5	0.455 .003	9.7 0.2	-5.0	14.6	
LWR11198	N	0.499 .007	-0.3 0.1	12.1	0.468 .002	6.9 0.1	0.0	15.4	
LWR11199	T	0.500 .007	-1.3 0.6	15.5	0.436 .003	3.9 0.2	-1.6	16.4	
mean	-	0.511±.022	-0.8±0.4	13.8	0.453±.013	7.1±2.4	-4.2	14.2	
LWR 9758	N	0.525±.010	-0.1±0.2	40.3	0.427±.011	1.8±0.1	66.9	43.0	

Image	type	2599 Å (order 89)		
		EW (Å)	% residual	V_r
LWR11196	N	0.337±.002	9.5±0.0	11.7
LWR11197	T	0.340 .004	12.2 0.5	11.7
LWR11198	N	0.349 .006	10.8 0.4	11.7
LWR11199	T	0.324 .006	12.0 0.0	11.1
mean	-	0.338±.010	11.1±1.2	11.6±0.3
LWR 9758	N	0.318±.002	13.8±0.1	42.1

Note on velocities: The velocities were corrected for earth and spacecraft motions. The difference of more than 25 km/sec between LWR9758 and the images LWR11196-11199 appears to be a good example of thermal shifts. LWR9758 was taken with THDA = 17.2°C, and was processed with the mean calibrations. LWR11196-11199 were taken at THDA ~ 12.5°C, and were processed with the new processing scheme which includes empirical THDA corrections (Thompson, Turnrose, Bohlin IUE Newsletter 15, p.8). Figure 14 on p. 51 IUE Newsletter No. 15 indicates that the wavelengths reported for LWR9758 would be too large by ~22 km/s, so its velocity should be decreased by this amount.

A.V. Holm

R. J. Panek

September 11, 1981

Wavelength (Å)	Velocity (km/s)	EW (Å)	EW (mÅ)
4101.0	1.51	0.15	0.15
4102.0	1.51	0.15	0.15
4103.0	1.51	0.15	0.15
4104.0	1.51	0.15	0.15
4105.0	1.51	0.15	0.15
4106.0	1.51	0.15	0.15
4107.0	1.51	0.15	0.15
4108.0	1.51	0.15	0.15
4109.0	1.51	0.15	0.15
4110.0	1.51	0.15	0.15

Wavelength (Å)	Velocity (km/s)	EW (Å)	EW (mÅ)
4111.0	1.51	0.15	0.15
4112.0	1.51	0.15	0.15
4113.0	1.51	0.15	0.15
4114.0	1.51	0.15	0.15
4115.0	1.51	0.15	0.15

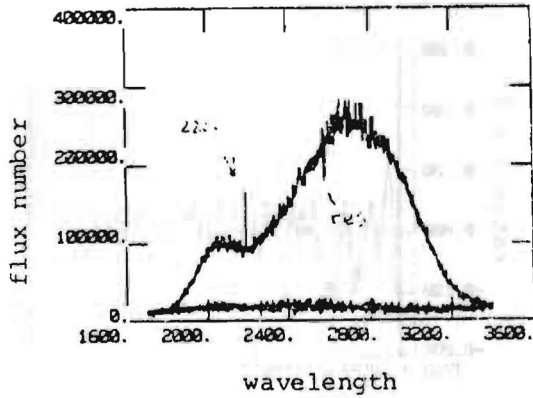
LOW DISPERSION TRAILED SPECTRA

FIG 1: Gross spectrum LWR10930

The hot pixel near 2200 Å and a reseau mark are flagged.

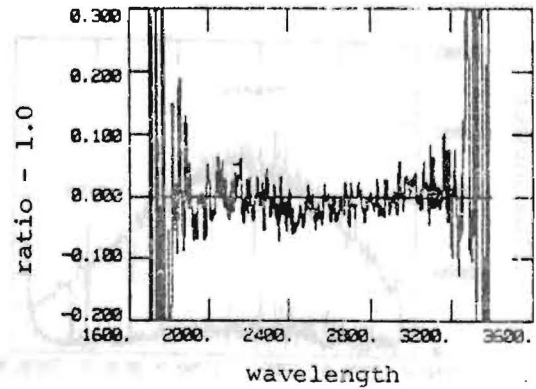


FIG 2: Ratio of test read/normal read
LWR10930/LWR10931 smooth 5 pixels

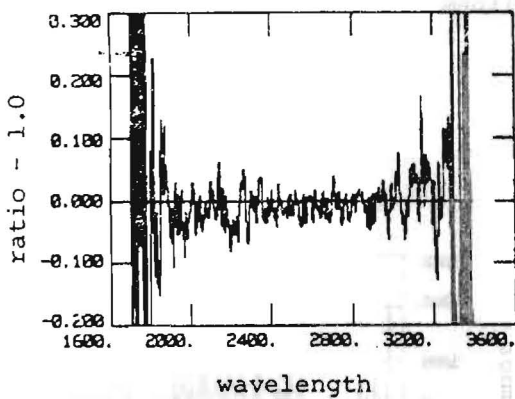


FIG 3: Ratio of test read/normal read
LWR10932/LWR19033 smooth 5 pixels

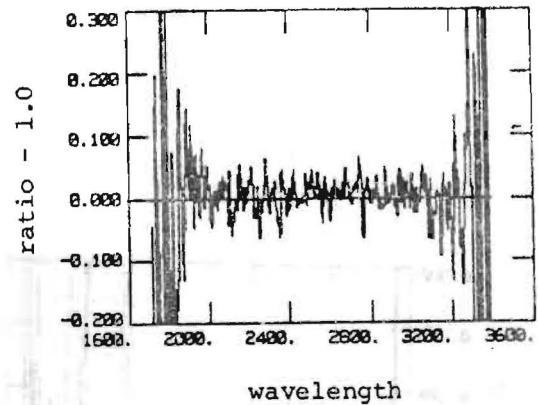


FIG 4: Ratio of normal read/normal read
LWR10933/LWR10931 smooth 5 pixels

Illustrates the expected level of repeatability.

HIGH DISPERSION SPECTRA

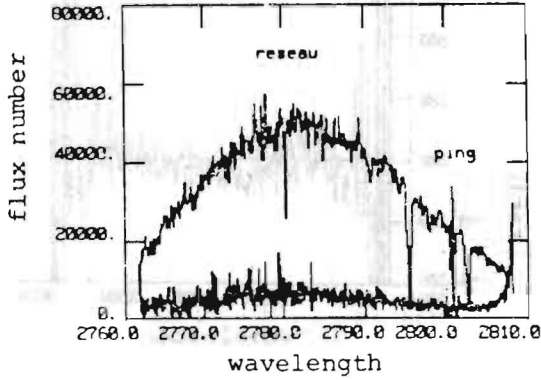


FIG 5: Order 83 Gross spectrum and background LWR11196

The MgII lines are evident at 2795, 2803 A. A reseau mark and the ping are marked.

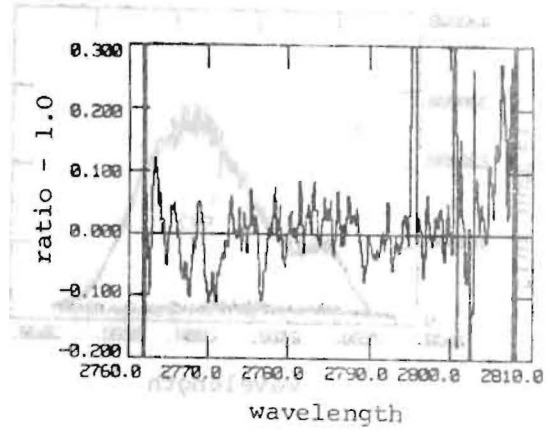


FIG 6: Order 83 Ratio Test read/normal read LWR11197/LWR11196

The effect of the ping is seen near 2801 A. The ratio also differs markedly from unity at the MgII lines.

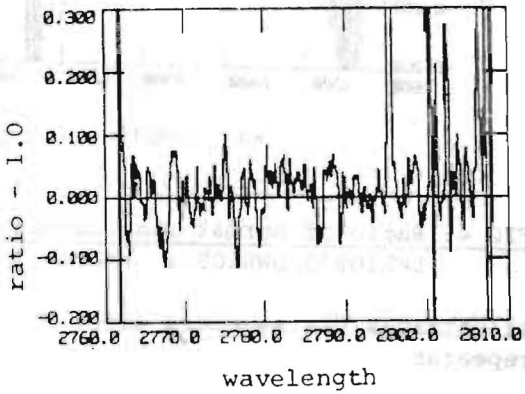


FIG 7: Order 83 Ratio Normal read/normal read LWR11198/LWR11196

Again the ping is apparent, and the ratio is extreme at the MgII lines.

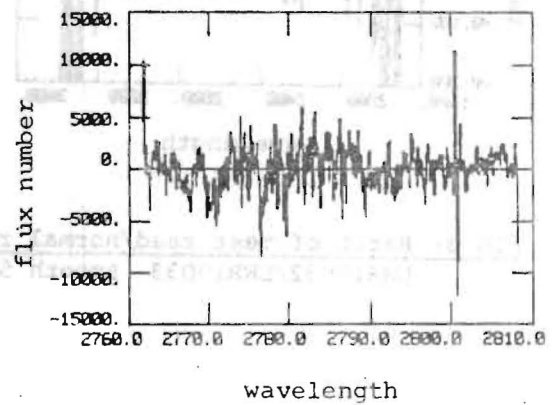


FIG 8: Order 83 Difference Test read - normal read LWR11197 - LWR11196

The ping is evident, but the difference is smooth across the MgII lines. This indicates that the anomalous ratio there is due to the noise inherent in very deep lines.

S/N CHARACTERISTICS OF LWP AND LWR CAMERAS
AT HIGH DISPERSION

M. Barylak, ESA/VILSPA

SUMMARY

A comparison between the signal-to-noise (S/N) ratios of the LWP and the LWR camera at high dispersion is presented. Two methods were used to obtain these ratios: a polynomial fit of the net spectra and a simplified Fourier analysis. The LWP, compared with the LWR, provides a better S/N longward of 2500 Å. The opposite happens shortward of this wavelength.

The data reduction was carried out with the Tololo-Vienna Interactive Image Processing System at VILSPA.

INTRODUCTION

High resolution spectra of the three standard stars HD93521, BD + 28°4211 and BD + 75°325 were used for the investigation of the noise characteristic of the LWP camera. The image numbers and the observational data are given in Table 1.

TABLE I: IUE Images used

:Image No.	:Object	:Exp.time	:Date	:Observer
:LWR 13186	:BD+75°325	:2160 s	:07May82	:Cassatella
:LWP 1464	:BD+75°325	:1960 s	:25Jan82	:Wamsteker
:LWR 5024	:BD+28°4211	:4800 s	:13Jul79	:Beeckmans
:LWP 1441	:BD+28°4211	:4080 s	:14Jan82	:Patriarchi
:LWR 9953	:HD 93521	:270 s	:19Feb81	:Bianchi
:LWP 1280	:HD 93521	:240 s	:19Feb81	:Bianchi

Fourteen orders were chosen at intervals of approximately 100 Å. The net spectra were resampled at constant intervals using linear

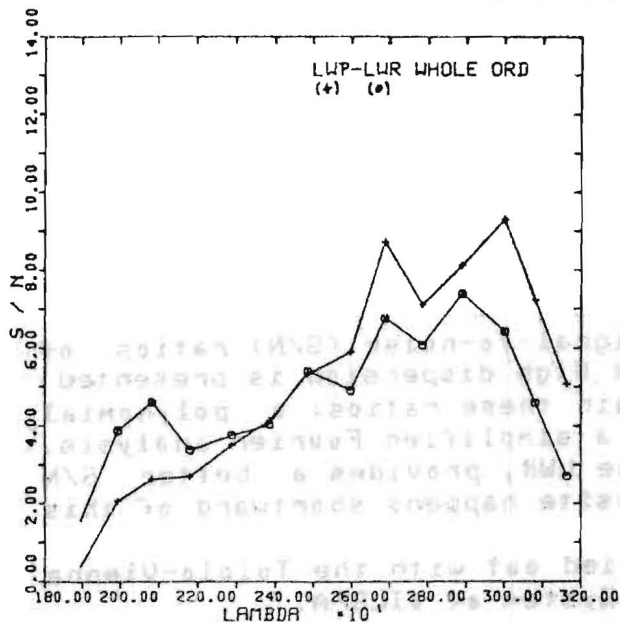


Figure 1. S/N ratio as obtained by fitting the whole order with a polynomial of second degree including negative values at the end.

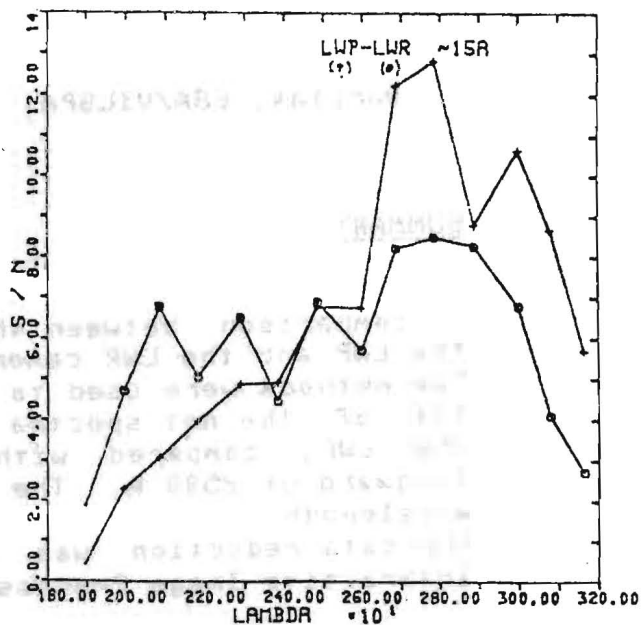


Figure 2. Same as figure 1, but here only the middle part of the individual order was fitted.

interpolation. This procedure has certainly reduced the noise contents of the spectra somewhat, but this is not significant. Two methods were applied to obtain the S/N ratio for each individual order: a polynomial fit and a simplified Fourier analysis.

POLYNOMIAL FIT

In this case the net spectrum was fitted by a polynomial of second degree. This fit was used to determine the S/N-ratio by two different methods. One using the whole order fit and the other using only the middle part of each order. This served to analyse the consequences of the inclusion of the negative values at the ends of the orders, which were excluded by the use of the truncated orders. The mean value of each range fitted was taken as representative of the signal and the square root of the reduced chi square $\chi = [(Y - Y(\text{fit}))^2 / n]^{1/2}$, where n is the degree of freedom (which is the number of data points minus the number of coefficients minus 1), was taken as that one for the noise.

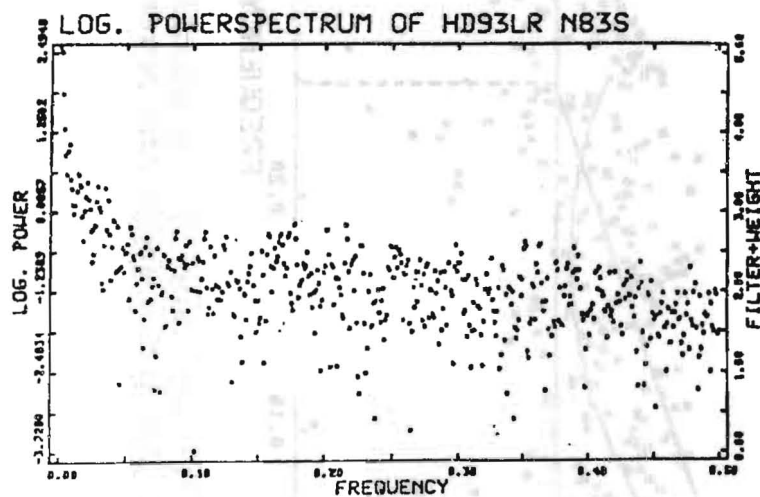
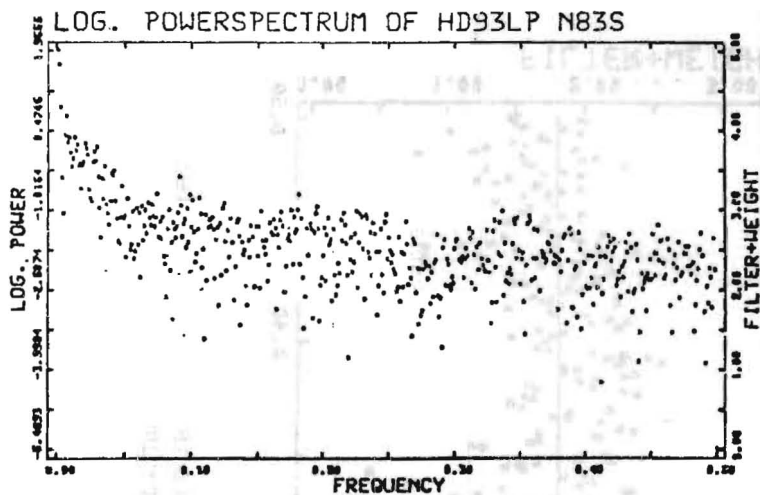


Figure 3. The logarithmic power spectra of order 83 for the LWP camera (top) and the LWR camera (bottom) versus Nyquist frequency (see text).

The results are shown in Fig. 1 (whole order fit) and Fig. 2 (fit of the middle part of an order). There the average of the S/N ratio of the three stars are presented. Although LWP has a worse noise characteristic from 1800 Å to 2400 Å, it behaves better than LWR longward of 2500 Å (see also LWP User's Guide).

FOURIER ANALYSIS

In order to prove the results obtained by the method above, I use a Fourier analysis of the net spectra of the star HD 93521 employing the Fourier-package of the Tololo-Vienna Image Processing System. The logarithmic power spectrum of each order was plotted against the Nyquist frequency N_y ($= 1/2 \Delta x$, where Δx is the distance of the data points).

The following two assumptions were made: 1, all the signal is contained in the lower frequencies (i.e. from 0.0 to 0.25 N_y) and 2, the higher frequencies (from 0.25 to 0.25 N_y), contain the noise only. Then the area under the power spectrum from 0.0 to 0.25 N_y is representative of the signal and the area under the spectra from 0.25 N_y represents the noise.

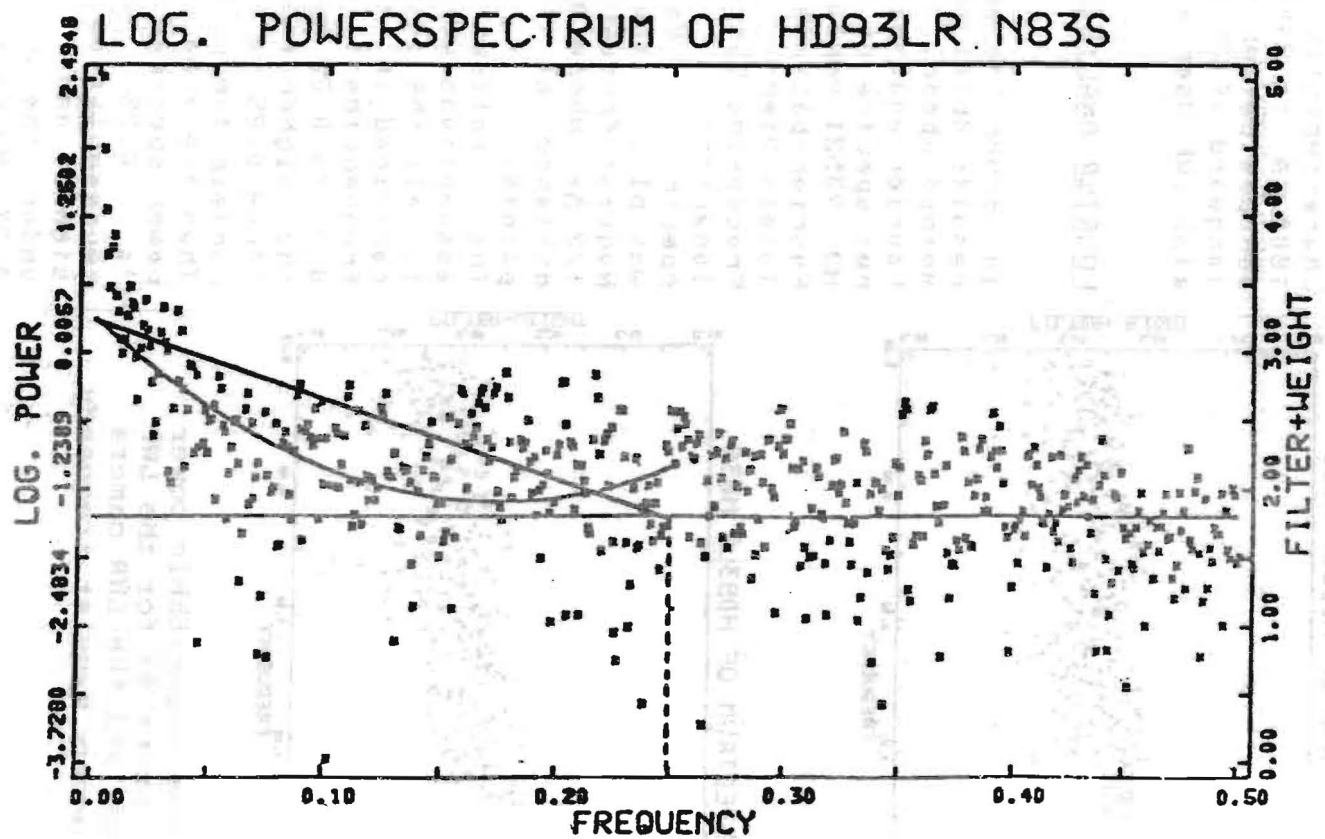


Figure 4. Illustration of the simplifications done in order to compute the areas under the power spectrum (see text).

As one can see in Fig. 3 the computation of the real area under the power spectrum is not an easy task. Therefore some simplifications were made. The power spectrum from 0.0 to 0.25 Ny was first approximated by a Voigt function, which was subsequently substituted by a straight line (see Fig. 4). The part from 0.25 to 0.5 Ny of the power spectrum was fitted by a constant (assuming "white noise"). The results (Fig. 5) of this method confirm the results obtained with the polynomial fitting approach.

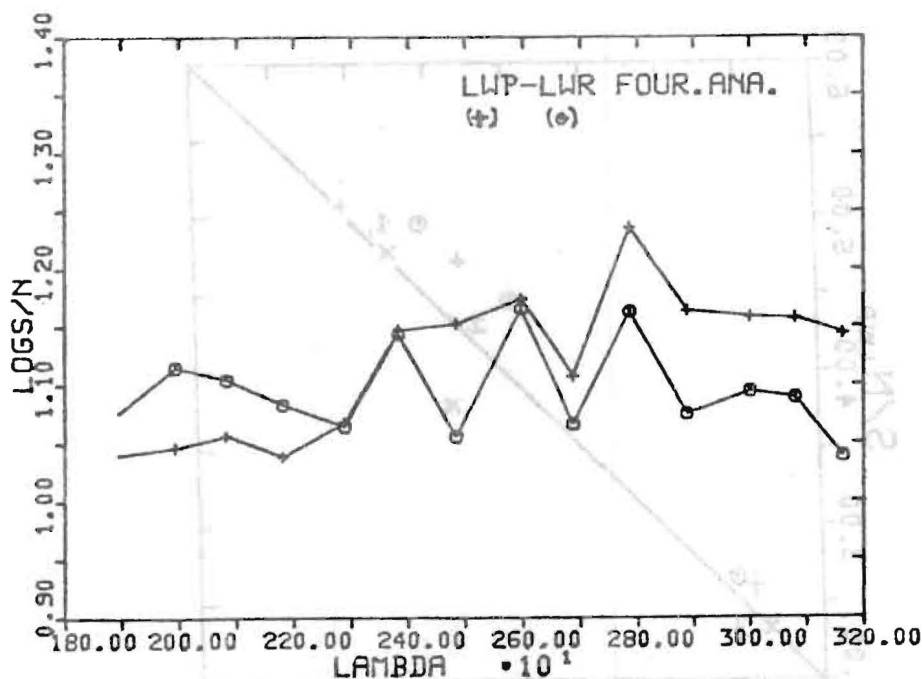


Figure 5. Result of the simplified Fourier analysis. These results are in good agreement with those obtained by the polynomial fit shown in figure 1.

S/N AT THE MgII LINES

The signal-to-noise ratios of LWP and LWR at the two resonance lines Mg II 2795.5 and Mg II 2802.7 are of special interest.

A polynomial fit, as described above, was made over an interval of 4 Å centered at these two lines.

The Mg II 2802.7 lies close to the end of order 83, therefore the S/N ratios for this line were computed at the end of order 83 (+) and at the beginning of order 82 (x)

(see Fig. 6). The S/N ratios of the Mg II 2808.7 line of these two different orders are not comparable, because they represent the characteristics of a completely different area of the detector. Fig. 6 shows a comparison of the S/N ratios of LWP and LWR as obtained for the same three standard stars. As one can see for the Mg II 2795.5 line of order 83 (o) the ratios lie above the 1:1-line in favor of the LWP. The same holds for the Mg II 2802.7 line of order 82 (x), LWR seems to have an equal (in case of star BD + 75° 325 (2,) even a better) noise characteristic than LWP.

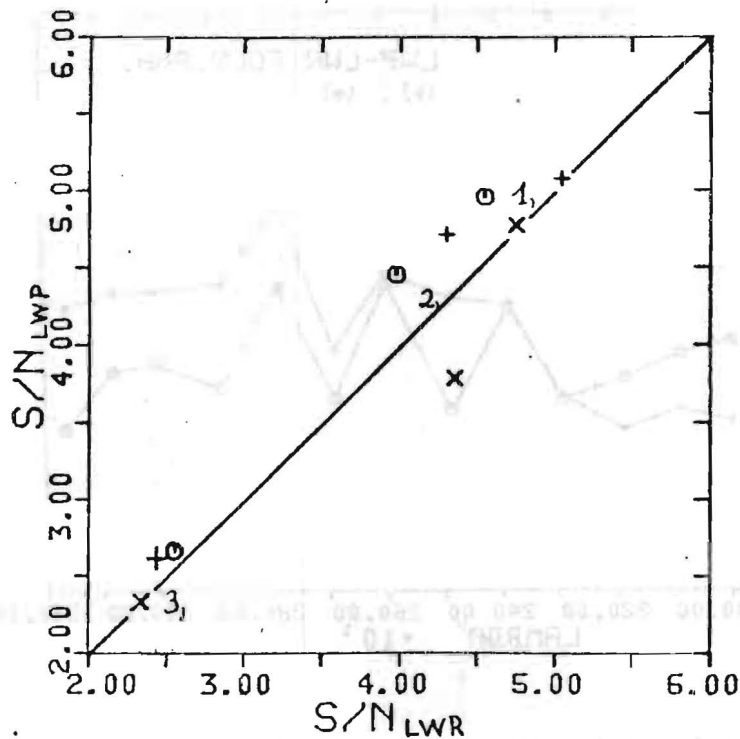


Figure 6. Comparison of the S/N ratios of the LWP and LWR cameras at the position of the Mg II lines for the stars BD +28° 4211 (1), BD +75° 325 (2) and HD 93521 (3). See also text.

CONCLUSION

It appears, that LWP is mainly useful for spectral studies in the wavelength range from 2500 to 3200 Å. In this

region the S/N in the LWP is about a factor of 1.4 better than in LWR. Conversely the LWR seems to be more appropriate for studies shortward of 2500 Å, where it is clearly better than the LWP both in terms of S/N and of sensitivity. For studies of the Mg II lines of order 83 again the usage of LWP is advisable.

ACKNOWLEDGEMENT

I would like to thank A. Cassatella and D. de Pablo for helpful discussions and W. Wamsteker for his corrections. I want to acknowledge the work of E. Torres, who made the first implementation of the TV system in VILSPA.

USE OF THE LWP CAMERA, AND ITS ABSOLUTE CALIBRATION

Over the last eighteen months the Project has invested considerable time in the calibration and study of the LWP camera. Much of the work has been completed, and the camera is now available on a routine basis to all Guest Observers. In this note we compare the properties of the two long wavelength cameras (See also ESA IUE Newsletter # 11), in order to help GOs decide which camera they should choose, and present the absolute calibration of the LWP camera (see also Barylak (this newsletter)).

In the Users Guide for the LWP camera (Settle, Shuttleworth and Sandford, 1981) a comparison of the two LW cameras in the low-dispersion mode shows that the LWP is both more sensitive and has better S/N characteristics longward of 2500 Å. Shortward of 2500 Å the LWR is the better camera. Figures 1 and 2 illustrate these properties. Other studies presented at the September 1982 3-Agency Meeting, VILSPA showed that at high dispersion the spectroscopic resolution is better in the LWP over most of the orders studied, except near 2800 Å and longward - where the resolutions are similar (see Figure 3, and Barylak loc.cit). The LWP camera shows the same characteristic high frequency noise as the other cameras, and has the same sensitivity to the background radiation as the SWP camera. The LWP camera does not suffer from the narrow band of microphonic type distortion prevalent in the LWR camera.

However the LWP ITF table may not be as well defined as the LWR ITF, since it contains only two, rather than four images. Also, it has been used much less than the LWR camera over the lifetime of the IUE, so there is much less photometric data available for this camera.

GOs wishing to use the LWP camera should inform the Resident Astronomer during their training session. Both tracking stations keep each other informed of planned LWP usage, thereby minimizing the switches between the two LW cameras as well as saving time during operations. Only one switch to the LWP and back is allowed per shift. Some time will be lost to the user during the switch - in the worst case about 20 mins - although some of the time can be hidden in other satellite operations.

Over the last year, both Observatories have been acquiring observations of standard stars to calibrate the LWP camera, and a provisional curve was presented at the 3-Agency meeting. Although a small amount of work still needs to be done on verification of the absolute

calibration, we present the data here, so that GOs can use it in their observations. The calibration has been included within IUESIPS by the end of October. The full details of the work will be published elsewhere.

The procedure used to determine the sensitivity curve of the LWP camera was to establish its overall shape, using trailed images of bright stars having well-established fluxes. To fix its absolute value we used fainter stars which can be accurately timed during exposure with IUE. This method is the same as that used in the revision of the absolute calibration of the SWP and LWR cameras and is independent of the LWR camera. To determine the shape, 12 trailed spectra of 4 HD stars (3360, 34816, 155763 and 214680) were used, whilst the absolute value was fixed with 23 spectra of 4 other stars (HD 60753, HD 93521, BD +28° 4211 and BD +75° 325). The resulting mean sensitivity curve, weighted according to the square-root of the number of individual spectra, is shown in Figure 4, and given in table I in 25 A bins for a wavelength range from 1900-3200 A.

As a first check on this calibration, we have compared fluxes obtained from both the LWP and LWR observations of the same star, finding the result that the two cameras are internally consistent, i.e. both cameras give the same fluxes to within reasonable errors (10%). There is a tendency for the LWP to give slightly large fluxes, of the order of 5%, compared to the LWR. Taken overall, the two calibrations agree well.

J.C. Blades
A.C. Cassatella

GOs wishing to use the LWP camera should refer to the Radiation Astronomer during their training session. Both tracking stations keep each other informed of planned LWP usage, thereby minimizing the switches between the two cameras as well as saving time during operations. Only one switch to the LWR and back is allowed per shift. Some time will be lost to the user during the switch - in the worst case about 28 min - although some of the time can be hidden in other satellite operations.

Over the last year, both Observatories have been making observations of standard stars to calibrate the LWP camera, and a provisional curve was presented at the 3-point meeting. Although a small amount of work still needs to be done on verification of the absolute

TABLE I
ABSOLUTE CALIBRATION OF THE LWP CAMERA AT LOW DISPERSION

Lambda (A)	S_{λ}^{-1}	Lambda (A)	S_{λ}^{-1}
1900	11	2600	0.583
1925	4.13	2625	0.539
1950	3.04	2650	0.506
1975	2.59	2675	0.507
2000	2.44	2700	0.502
2025	2.17	2725	0.498
2050	1.97	2750	0.501
2075	1.96	2775	0.500
2100	1.98	2800	0.511
2125	1.96	2825	0.520
2150	1.99	2850	0.540
2175	2.05	2875	0.549
2200	1.95	2900	0.565
2225	1.93	2925	0.604
2250	1.81	2950	0.663
2275	1.62	2975	0.704
2300	1.50	3000	0.795
2325	1.37	3025	0.909
2350	1.26	3050	1.09
2375	1.14	3075	1.25
2400	1.02	3100	1.48
2425	0.947	3125	1.79
2450	0.864	3150	2.15
2475	0.804	3175	2.70
2500	0.730	3200	5.98
2525	0.679		
2550	0.624		
2575	0.599		

$$S_{\lambda}^{-1} : 10^{-14} \text{ erg cm}^{-2} \text{ A}^{-1} \text{ FN}^{-1}$$

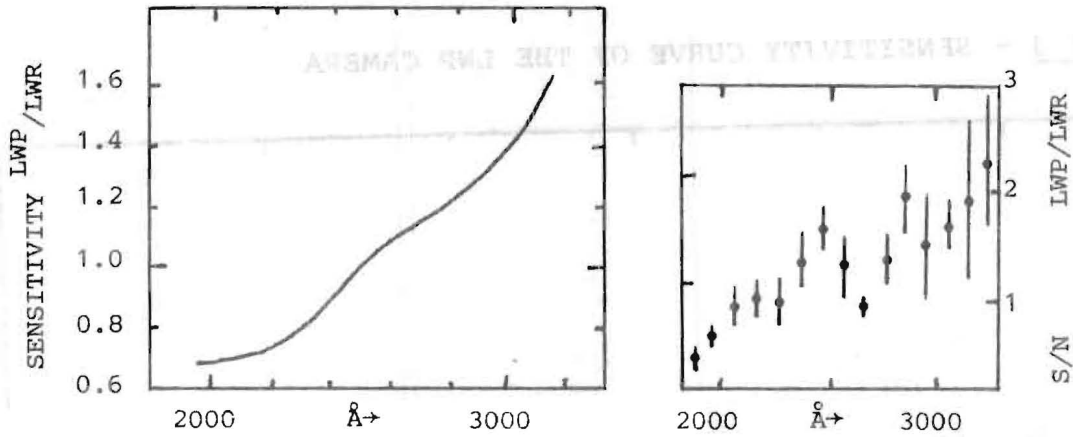


FIGURE 1 (a & b) - Comparison of the sensitivity of the S/N ratio for the two long wavelength cameras (Settle, Shittleworth, Sanford, 1981)

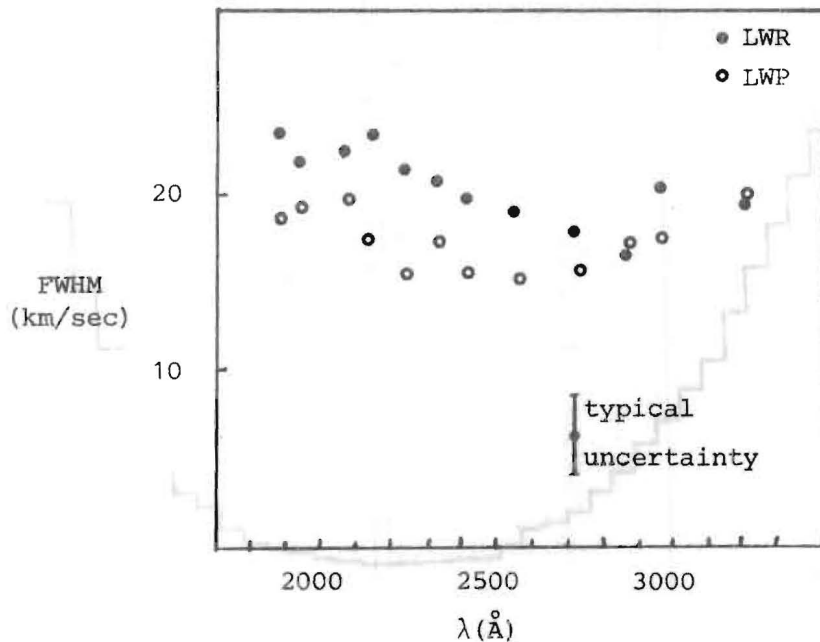
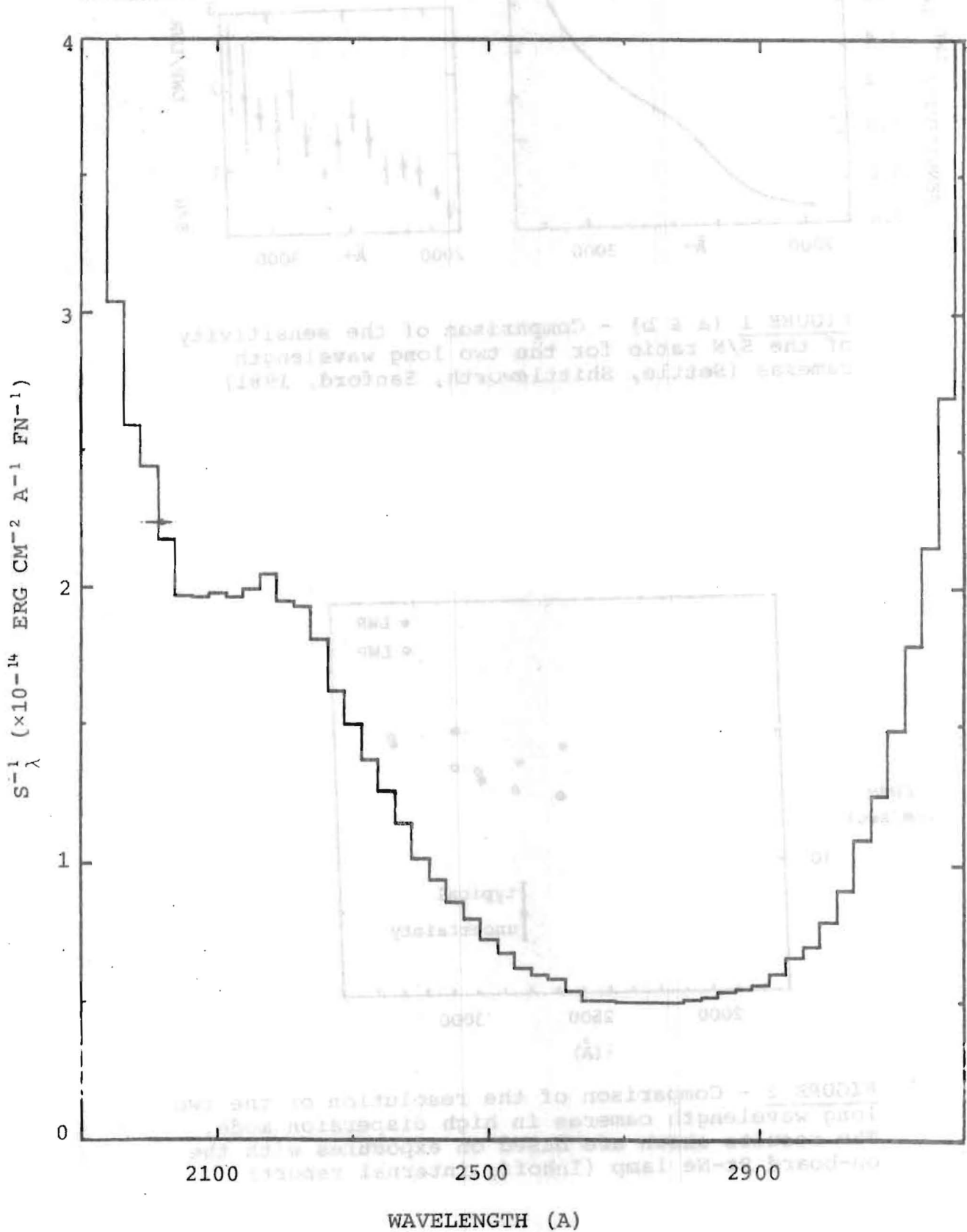


FIGURE 2 - Comparison of the resolution of the two long wavelength cameras in high dispersion mode. The results shown are based on exposures with the on-board Pt-Ne lamp (Inhoff, internal report)

FIGURE 3 - SENSITIVITY CURVE OF THE LWP CAMERA



ABSOLUTE CALIBRATION OF IUE HIGH RESOLUTION SPECTRA: CHANGES WITH THE NEW SOFTWARE

1. INTRODUCTION

High resolution spectra of point sources obtained through the spectrograph's large entrance apertures can be calibrated in terms of absolute fluxes using the high resolution calibration curves by Cassatella, Ponz and Selvelli (1981).

This calibration however, is only applicable to spectra processed with the software available at GSFC before November 10, 1981 and at VILSPA before March 11, 1982. At the above dates a new high resolution data processing software was installed at both IUE ground stations.

The new software, documented by Bohlin and Turnrose (1982) and references therein, makes use of substantially better geometric and photometric correction procedures. It also allows for a better registration of the orders, providing a more precise matching of the order's center with the wavelength dispersion overlays. Moreover, the slit height is optimized as a function of the order width and separation, instead of being fixed to about 6.4 pixels (for point source spectra) as in the old software. These changes, but in particular the upgraded precision in localizing the orders and the background in the images, have the global effect to increase the net flux extracted from the higher spectral orders (at the short wavelength ends of the cameras).

In the present report the influence of the new software on the high resolution calibration is studied, and preliminary results are provided.

2. CALIBRATION SAMPLE AND DATA ANALYSIS

Two pairs of low-high resolution spectra of the same star are used for each camera to redetermine the calibration factors C defined by Cassatella et al. (1981). These are SWP 9842 (low) and SWP 9843 (high) for BD +75°325; SWP 8703, SWP 8704, LWR 8703 and LWR 8704 for HD 60753.

The results were verified by taking the ratio of the spectra processed with the new and old software. This provides directly the corrections to be applied to the old C_{λ} curves. The smoothed calibration curves are shown in

Figure 1 and Figure 2 for the SWP and LWR camera, respectively, together with the previous curves in Cassatella et al..

The values are also reported in Table 1.

3. RESULTS AND DISCUSSION

The internal consistency of the new high resolution calibration, although based on a smaller sample of spectra, is similar to that of the old one, i.e. about 10% shortward of 2200 Å and about 5% longward of these wavelengths.

Examples of the new absolute calibration applied to high resolution spectra processed with the new software are given in Figure 3 and 4 for both the SWP and LWR Cameras.

In Figure 3a the calibrated high resolution spectrum of HD 187473 (from SWP 8280) is compared with a low resolution spectrum (SWP 8279) of the same target after rebinning both data at 2Å intervals. The corresponding r.m.s. deviation is about 4%. A slightly better accuracy is obtained in the case of BD +28° 4211 (using SWP 5778 and SWP 5779), as shown in Figure 3b. A similar comparison for the LWR camera is presented in Figure 3c for BD +75° 325 using LWR 8305 and LWR 8304. The r.m.s. deviation is about 6%. These comparisons are quite satisfactory although the selected spectral regions, corresponding to high orders, are the most sensitive to errors. Better precisions are obtained at longer wavelengths. This is shown in Figure 4, where the original LWR high resolution spectrum of HD 144668 is compared with a low resolution spectrum taken close in time, in a region around 2580 Å. The r.m.s. deviation is about 3% in this case.

It is clear from Figures 1 and 2 that the new calibration factors C_λ are systematically lower at the short wavelength end of the cameras than in the old software. This is due to the gain in extracted flux expected as a consequence of the improved data extraction. In particular, the gain in extracted net flux is about 10% around order 110 in both cameras (near 1250 Å in the SWP and near 2100 in the LWR), and decreases regularly with decreasing order number. This is in good agreement with the new software evaluation tests reported by Bohlin and Turnrose (1982). Longward of 1450 Å in the SWP camera and 2425 Å in the LWR, the new software does not show any significant gain compared with the old software. As a consequence, the new and old curves C_λ coincide longward of

these wavelengths.

Concerning the absolute calibration of emission line sources with faint or no continuum, the same equations hold as for the old software, i.e.:

$$C_{\lambda} = 228.009 - 0.0755 \lambda \text{ for } 1400 \leq \lambda \leq 1975 \text{ \AA}$$

$$C_{\lambda} = 167.099 - 0.0229 \lambda \text{ for } 2300 \leq \lambda \leq 3100 \text{ \AA}$$

These equations fit very well the new calibration for continuous sources longward of 1575 \AA in the SWP, and of 2500 \AA in the LWR camera.

Cross checks of the above equations, using spectra of RR Tel, confirm their validity.

A.Cassatella

D.Ponz

P.L.Selvelli

REFERENCES

Cassatella, A., Ponz, D., Selvelli, P.L., 1981, ESA IUE Newsletter No. 10, p. 31, and NASA IUE Newsletter No. 14, p. 170

Bohlin, R.C., Turnrose, B.E., 1982, ESA IUE Newsletter No. 13, p. 14 and NASA IUE Newsletter No. 18, p. 29

TABLE 1 - CALIBRATION FACTORS C_λ

Lambda (A)	New	Old	Lambda (A)	New	Old
1250	205	230	1925	230	292
1275	192	208	1950	206	259
1300	178	193	1975	190	229
1325	168	176	2000	177	207
1350	158	163	2025	168	191
1375	148	152	2050	159	180
1400	142	143	2075	153	171
1425	136	136	2100	146	165
1450	131		2125	142	159
1475	126		2150	138	153
1500	122		2175	134	149
1525	118		2200	131	143
1550	114		2225	129	139
1575	110		2250	126	136
1600	108		2275	124	132
1625	105		2300	122	129
1650	103		2325	120	126
1675	101		2350	119	122
1700	100		2375	118	120
1725	98		2400	117	118
1750	96		2425	116	116
1775	94		2450	115	
1800	92		2475	114	
1825	90		2500	113	
1850	88		2525	112	
1875	86		2550	110	
1900	84		2575	109	
1925	82		2600	108	
1950	81		2625	107	
1975	80		2650	106	
			2675	105	
			2700	104.5	
			2725	104.0	
			2750	103.5	
			2775	103.0	
			2800	102.5	
			2825	102.0	
			2850	101.5	
			2875	100.5	
			2900	100.2	
			2825	100.0	
			2950	99.0	
			3000	98.5	
			3025	98.0	
			3050	97.5	
			3075	97.0	
			3100	96.5	

FIGURE CAPTIONS

FIGURE 1:

C_λ curve applicable to SWP high resolution spectra of continuous sources processed with the new software (crosses) and the old software (dots). The two curves coincide longward of 1450 Å.

FIGURE 2:

C_λ curve applicable to LWR high resolution spectra of continuous sources processed with the new software (crosses) and old software (dots). The two curves coincide longward of 2425 Å.

FIGURE 3 (a,b and c) :

Comparison between a low resolution (thick line) SWP spectrum and a calibrated high resolution spectrum (thin line) of the stars HD 187473 and BD +28°4211, both resampled at 2 Å intervals. Figure 3c shows the same comparison for BD +75°325.

FIGURE 4:

Calibrated high resolution spectrum of HD 14466B compared with a low resolution spectrum (dots) taken close in time.

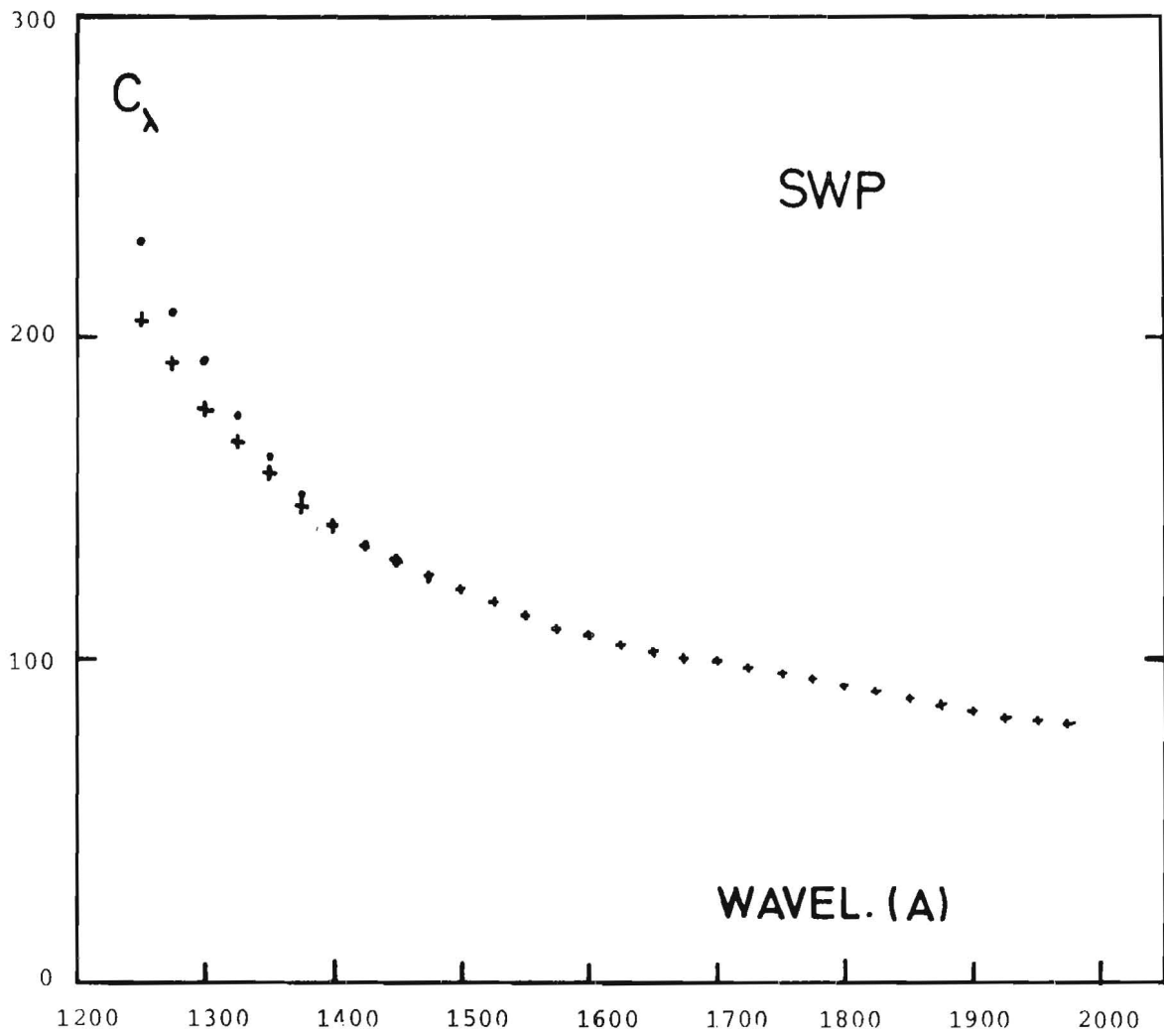
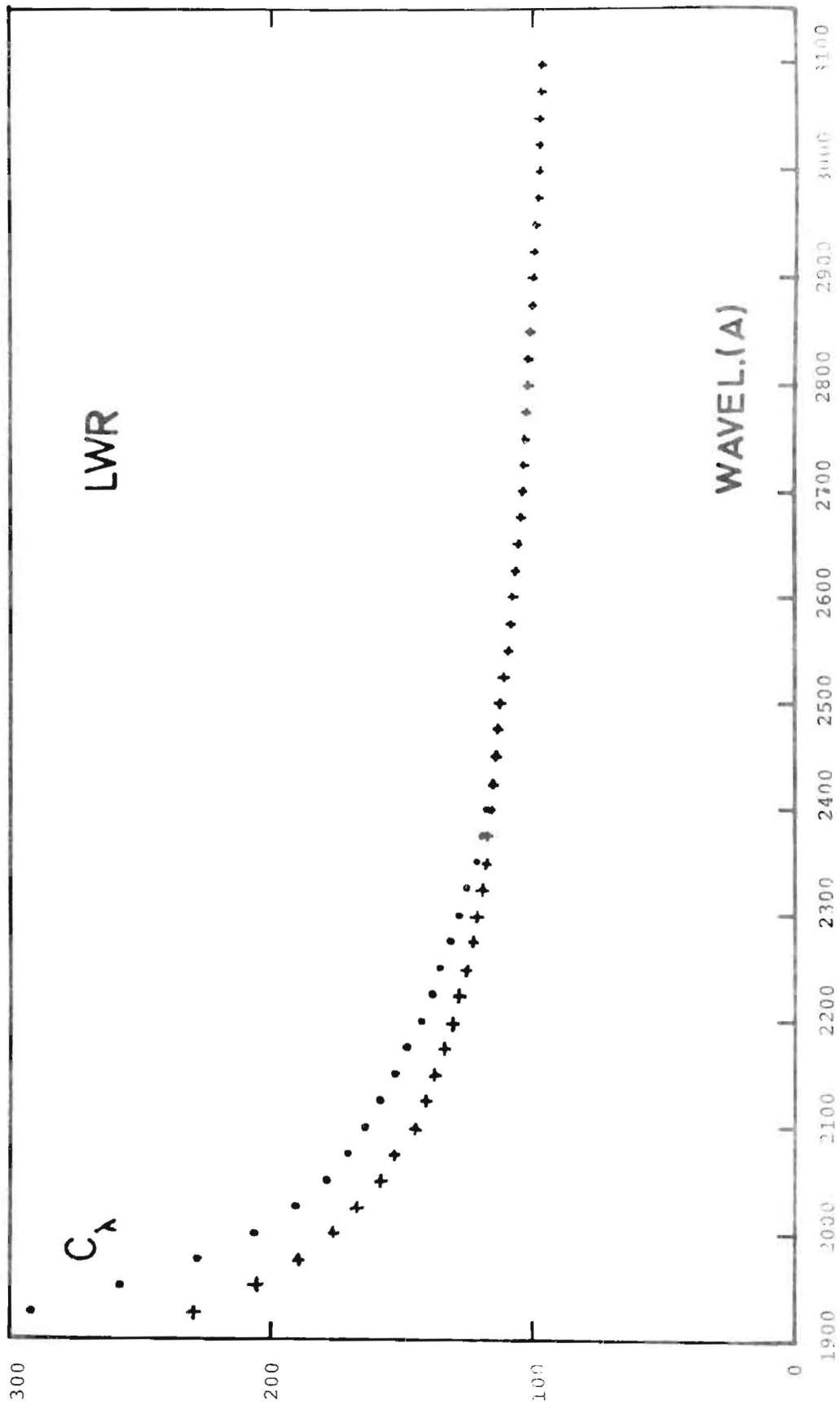


FIGURE 1

FIGURE 2



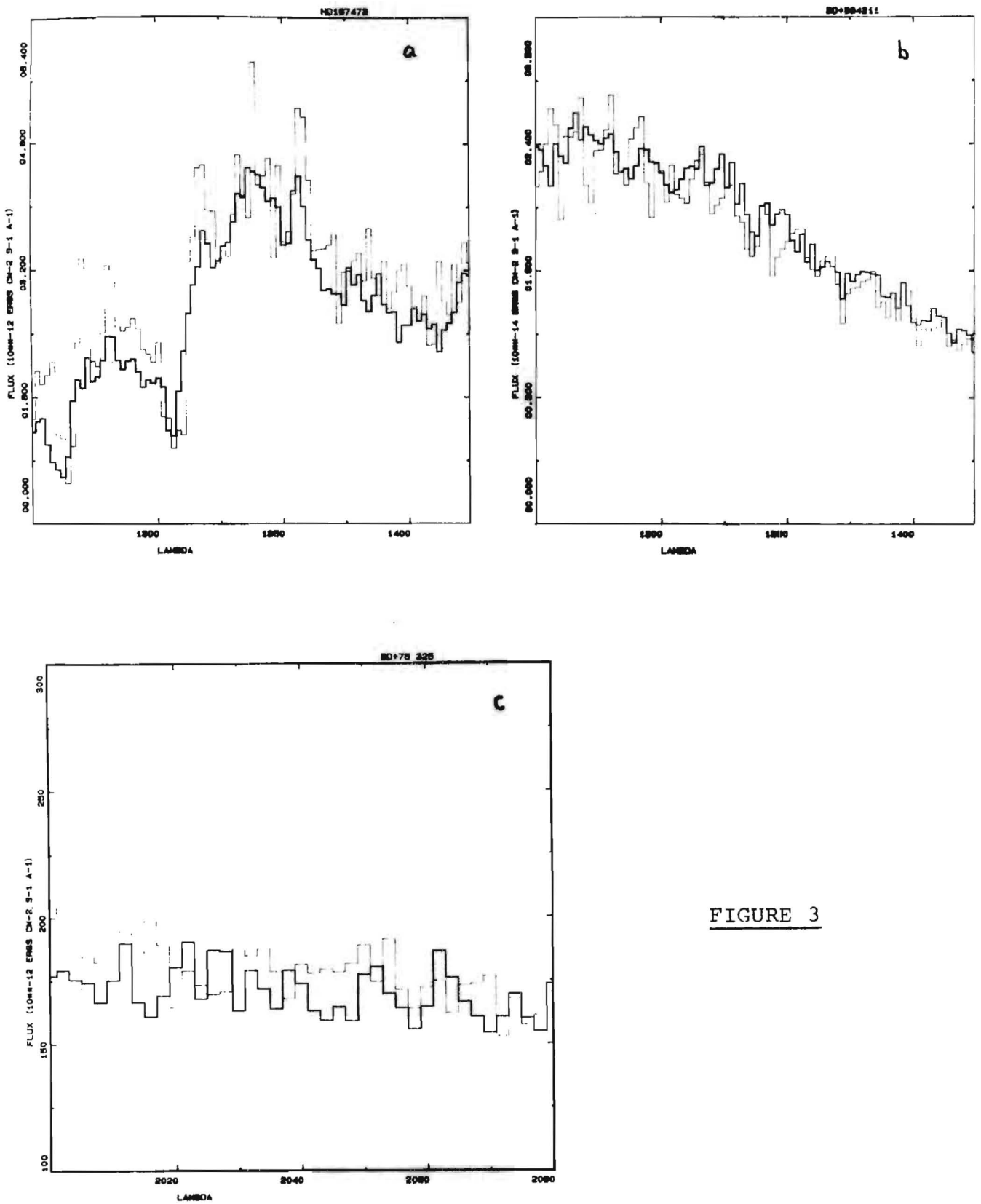


FIGURE 3

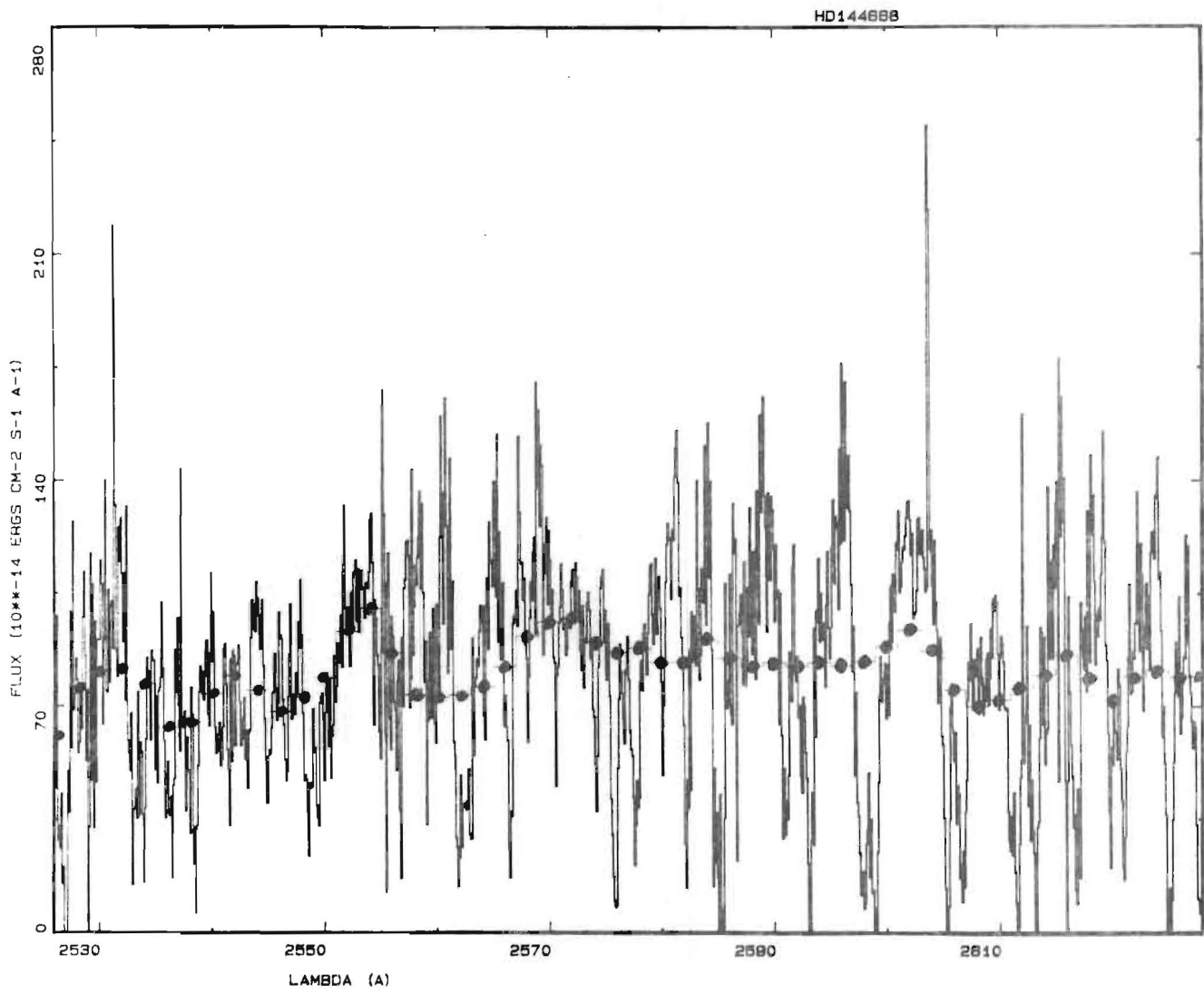


FIGURE 4

Interactive Facility for consulting the Merged Log of Observations
at VILSPA

1. Introduction

Since the 1st. of October '82, a new facility is at the disposal of the Guest Observers, Resident Astronomers and Scientific Visitors of VILSPA.

This new facility enables the visitor to use a computer terminal to communicate in a conversational way with a file of Merged Log of observations. The type of questions allowed is powerful enough to quickly retrieve any collection of data placed in such Merged Log.

At the moment, the system is in operation every day from 16.00 hrs. local onwards. Experience will advise whether or not to modify this schedule.

The facility is implemented around a Data Base Management Package which allows the application to operate with the data files without constraining the file design or its contents.

2. Merged Log Consultations

The Merged log file is organized in "Records" of 80 characters.

Each record describes an observation and is subdivided into "Fields", which are each one of the elements of the recorded observation.

The actual descriptors of these fields are:

- NAM - Object name (up to 8 characters).
- CLA - Object class (2 digits).
- MAG - Object magnitud (up to 3 characters).

- RHO - Right Ascension hours coordinates.
- RMI - Right Ascension minutes coordinates.
- RSE - Right Ascension seconds coordinates.
- SIG - Declination sign (+ or -).
- DDE - Degrees Declination coordinates.
- DMI - Minutes Declination Coordinates.
- DIS - Dispersion Image (H or L).
- CAM - Camera (1, 2, 3 or 4).
- NIM - Image Number (up to 5 digits).
- APE - Aperture (S or L).
- LST - Large Aperture status (O or C).
- DAY - Day of Observation.
- MON - Month of Observation (3 characters).
- YEA - Year of Observation.
- EHO - Exposure start hours.
- EMI - Exposure start minutes.
- ESE - Exposure start seconds.
- ELM - Exposure length minutes (3 digits).
- ELS - Exposure length seconds.
- OBS - Observing program (5 characters).

Our interactive facility allows to ask questions about any of these fields or any boolean combination of them. The response is given in a pre-specified format.

The questions to the Merged Log are structured in the form:

'COMMAND' 'CRITERIA'

where the 'COMMANDS' allowed to the user are:

- FI: Identify the set of records that meet certain criteria
- FIA: Extracts from the previously selected records the ones meeting certain criteria.

- FIO: Same as FIA (Find AND) but performing the 'OR' operation between previously selected records and the ones meeting the specified criteria.
- CO: Count: returns a count of the number of records meeting specified criteria.
- COA: Count + "AND" criteria (similar to FIA).
- COO: Count + "OR" criteria (similar to FIO).
- LK: Establishes start position to retrieve records in logical sequence order.
- GN: Obtain next record in the list.
- DR: Display a record.
- VIEW: Specify a display format.

and the 'CRITERIA' are boolean function constituted with the above mentioned "Field Descriptors".

A few examples will show the power of the system.

EXAMPLE 1: Display the records meeting the criteria:

- Camera is LWP
- Low Dispersion
- Object Classification is 99 (Nulls and Flat Field)
- Image Sequential Number higher than or equal to 1000.

The question to be asked is:

FI CAM=1 AND DIS=L AND CLA=99 AND NIM>1000.

The system will respond that he found 81 records.

On commanding DR VIEW:MERV02 (Display Record with the output format MERV02), the first record will be displayed.

Commanding GN (Get Next) will retrieve after every new "Carriage Return" the next record complying with the search criteria.

EXAMPLE 2: Let us assume that we are interested in collecting the observations made in high dispersion with the shortwave spectrograph to the object NGC 4151. The difficulty to overcome is the fact that the object might be coded under different names so that we can only rely on its coordinates. Furthermore, the recorded coordinates might differ by a small amount, so that, in conclusion, what we want is to find the high dispersion observations made to objects whose R.A. and Declination are around one of the recorded coordinate values of that object.

One way of proceeding could be as follows:

- First let us find the coordinates of this object:

```
FI NAM='NGC 4151'
```

The system will respond with

```
'115 RECORDS FOUND'
```

and the first one will be displayed.

Notice the coordinates R.A. = 12 08 00 and declination = + 39 41 00.

- Find now all records with coordinates 12 08 and 39 41 (i.e. within 60 seconds above these values):

```
FI RHO=12 AND RMI=08 AND DDE=39 AND DMI=41.
```

The system will respond

'207 RECORDS FOUND'

and the first one will be displayed.

(Notice there are more records than in the preliminar question).

The command

FIA CAM=3

will select from the 207 records the ones observed with SWP camera.

System responds with

'117 RECORDS FOUND'.

Now, the command

FIA DIS=H

will select (from the previous set) the observations in high resolution.

The system respond with

'5 RECORDS FOUND'

and the first one will be displayed. After subsequent 'Carriage Returns' the other 4 records will be also displayed.

Of course, after a little experience, an overall command like

FI RHO=12 AND RMI=08 AND DDE=39 AND DMI=41 AND CAM=3 AND DISP=H

would have performed the whole search.

3. Available Display Formats

The system offers more ample facilities than the ones described here. As a matter of fact the user can even create his/her own display format. For reference, it is included here a reduced list of the available formats (called 'views' or 'userviews', in IGCS jargon).

D. de Pablo, IGCS

APPENDIX B

VIEW:MERVO1

MERGE LOG														
OBJECT			COORDINATES									OBS. DATE		
NAME	CL	MAG	HOUR	MIN	SEC	DEG	MIN	CAM	IMAGE	AP	ST	DAY	MONTH	YEAR
34029	45	00	05	12	59	45	56	4	01022	S	0	09	FEB	78
EXPOSURE														
ST.		LENGTH		PROG.		COMMENTS								
HOUR	MIN	SEC	MIN	SEC										
22	02	00	001	20	CEJLL	GCOMMISSIONING PERIOD								

VIEW:MERVO2

MERGE LOG					
OBJECT ID.	+75	325	CLASS	16	
			MAGNITUDE	92	
	HR	MN	SC	I. M.	
RIGHT ASCENSION	08	04	43	DECLINATION	+75 06
DISPERSION	L				
CAMERA N.	4			IMAGE N.	01024
APERTURE	S			LARGE AP. STATUS	0
DATE OF OBSERVATION	10FEB78				
	START			LENGTH	
EXPOSURE	HR	MN	SC	MN.	SC.
	04	27	00	010	00
OBSERVER PROGRAM	HSSRH				
COMMENTS	GCOMMISSIONING PERIO				

VIEW:REPV01

415184	90120800+3941H401025S010FEB7804560006000	TRG	GCOMMISSIONING PERIO
--------	--	-----	----------------------

VIEW:REPV02

-OBJECT	CL	MG	RIGHT	ASC	DEC.	C	IMAGE	DATE	EXPOSURE	OBS
4151	84	120	12	08	00	+	39 41 L 4	01026 S 0	11 FEB 78	19 57 00 060 00 TRG

VIEW:REPV03

-OBJECT	CL	MG	RIGHT	ASC	DEC.	C	IMAGE	DATE	EXPOSURE
6826	71	104	19	43	27	+	50 24 L 3	01140 S 0	13 MAR 78 20 44 00 002 30

VIEW:REPV04

153919	59	65	17.00.32	-37.46	H	4	01027	S0	11FEB78	22 53 00 100 00 XSAKD.
--------	----	----	----------	--------	---	---	-------	----	---------	------------------------

IUE VILSPA PUBLICATIONS

Outburst spectra of UZ Serpenti, Echevarria, J., Jones, D.N.P., Wallis, R.E., Mago, S.K., Hassall, B.J.M., Pringle, J.E., Whelan, J.A.J., 1981, MNRAS, 122, 565.

An analysis of the Planetary Nebula NGC 2867, Aller, L.H., Keyer, C.D., Ross, J.E., O Mara, B.J., 1981, MNRAS, 122, 647.

UV observations of the Be star and X-ray binary, 4U 1145-61 (= HD 102567 = Hen 715) obtained with IUE, De Loore, C., Burger, M., Hensberge, H., Van Dessel, E.L., 1981, A.A., 104, 150.

Far UV investigation of 3 nuclei of Globular Clusters, Caloi, V., Cassatella, A., Castellani, V., Macchetto, F., Melnick, J., 1981, A.A., 103, 386.

UV spectroscopy of the Galactic Globular Cluster M5. Altamore, A., Angeletti, L., Capuzzo-Dolcetta, R., Giannone, P., 1981, A.A., 103, L11.

UV observations of two extreme pop. II stars: detection of chromospheric emission and mass loss, Spite, M., Caloi, V., Spite, F., 1981, A.A., 103, L11.

IUE and ground based spectroscopic observations of the S Dor- type LMC variable R71 during minimum state, Wolf, B., Appenzeller, I., Stahl, O., 1981, A.A., 103, 94.

A high resolution IUE spectrum of the G0-G5, Ia supergiant HR 8752, Stickland, D.J., Lambert, D.L., 1981, A.A., 102, 296.

Mass loss from O subdwarfs, Hamman, W.R., Gruschinske, J., Kudritzki, R.P., Simon K.P., 1981, 104, 249.

The line spectrum of Fe II seyfert I galaxy Akn 120, Kollatschny, W., Schleicher, H., Fricke, K.J., Yorke, H.W., 1981, A.A., 104, 198.

Far UV observations of late k and M type stars, Stickland, D.J., Sanner, F., 1981, MNRAS, 122, 791.

Water production models for comet Bradfield (1979X), Weaver, H.A., Feldman, P.D., Festou, M.C., A'Hearn, M.F., 1981, Ap. J., 251, 809.

IUE observations of the X-ray burst source 4U/M 1735-44, Hammerschlag-Hensberge, G., Mc Clintock, J.E., van Paradijs, J., 1982, Ap. J., 254, L1.

The chromospheric and the wind of the Herbig Ae star, AB Aurigae, Praderie, F., Talavera, A., Felenbok, P., Czarny, J., 1982, Ap. J., 254, 658.

IUE observations of NGC 4649, an elliptical galaxy with a strong ultraviolet flux, Bertola, F., Capaccioli, M., Oke, J.B., 1982, Ap. J., 254, 494.

Far-ultraviolet observations of MV Lyrae, Chiapetti, L., Maraschi, L., Tanzi, E.G., Treves, A., 1982, Ap. J., 258, 236

Ultraviolet spectroscopy of Phi Persei, Kitchin, C.R., 1982, MNRAS, 198, 457.

Interstellar extinction in the Perseus arm, Morgan, D.H., MaLachlan, A., Nandy, K., 1982, MNRAS, 198, 779.

IUE spectra of clumpy irregular galaxies, Benvenuti, P., Casini, C., Heidmann, J., 1982, MNRAS, 198, 825.

Ultraviolet spectra of planetary nebulae. VIII. The ClO abundance in the Ring Nebula, Flower, D.R., 1982, MNRAS, 199, 15P.

The physical state of the gas towards HD 93206, Welsh, B.Y., Thomas, C.K., 1982, MNRAS, 199, 385.

The interstellar spectrum of the supernova 1980 k in NGC 6946, Pettini, M., Benvenuti, P., Blades, J., Boggess, A., Boksenberg, A., Grewing, M., Holm, A., King, D., Panagia, N., Penston, M., Savage, B., Wamsteker, W., Wu, C., 1982, MNRAS, 199, 409.

Ultraviolet spectra of Planetary Nebulae - VI - NGC 7662, Harrington, J.P., Seaton, M., Adams, S., Lutz, J., 1982, MNRAS, 199, 517

Mass loss from Be stars derived from UV spectra, de Freitas Pacheco, J.A., 1982, MNRAS, 199, 591.

The physical conditions within the poly-polar nebula NGC 6302, Barral, J., Canto, J., Meaburn, J., Walsh, J.R., 1982, MNRAS, 199, B17.

Detailed observations of NGC 4151 with IUE - II. Variability of the continuum from 1978 February to 1980 May, including X-ray and optical observations, Perola, G.C., Boksenberg, A., Bromage, G.E., Clavel, J., Elvis, M., Elvis, A., Gondahlekar, P.M., Lind, J., Lloyd, C., Penston, M.V., Pettini, M., Snijders, M.A.J., Tanzi, E.G., Tarenghi, M., Ulrich, M.H., Warwick, R.S., MNRAS, 200, 293.

Ultraviolet spectra of Planetary Nebulae. VII. The abundance of carbon in the very low excitation nebula He 2-131, Adams, S., Seaton, M.J., 1982, MNRAS, 200, 7P.

Infrared, optical and ultraviolet observations of TT Ari, Jameson, R.F., King, A.R., Sherrington, M.R., 1982, MNRAS, 200, 455.

A study of element depletions in interstellar gas, Phillips, A.P., Gondhalekar, P.M., Pettini, M., 1982, MNRAS, 200, 687.

IUE observation of UV absorption in the spectrum of the C2 white dwarf L 1363-3, Vauclair, G., Weidemann, V., Koester, D., 1982, Astron. Astrophys., 109, 7.

Abundances in the Planetary Nebula NGC 6853, Pottasch, S.R., Gilra, D.P., Wesselius, P.R., 1982, Astron. Astrophys. 109, 182.

UV, optical and IR observations of the Cepheid R Muscae, Eichendorf, W., Heck, A., Caccin, B., Russo, G., Sollazo, C., Astron. Astrophys. 109, 274.

The pulsation of the outer layers of the Beta Cephei Star T Sco, Burger, M., de Jager, C., van den Oord, G.H.J., 1982, Astron. Astrophys. 109, 289.

Magnetic structure in Cool stars. V. Chromospheric and transition region emission from giants, Orange, B.J., Zwaan, C., Middelhoop, F., 1982, Astron. Astrophys. 110, 30.

The interacting early-type contact binary SV Centauri, Drechsel, H., Rahe, J., Wargau, W., Wolf, B., 1982, Astron. Astrophys. 110, 246.

UV and visible photometry of the brighter Pleiades Stars, Golay, M., Maun, N., 1982, Astron. Astrophys. Suppl. Ser. 47, 547.

Analysis of the IUE and Optical Spectra of the Peculiar Be star HD 87643, de Freitas Pacheco, J. A., Gilra, D.P., Pottasch, S., Astron. Astrophys. 108, 111.

The ultraviolet spectrum of the Old Novae HR Del, GK Per, RR Pic, and RS Oph, Rosino, L., Bianchini, A., Rafanelli, P., 1982, Astron. Astrophys. 108, 243.

Spectral analysis of the OB subdwarf HD 149382, Baschek, B., Kruditzki, R.P., Scholz, M., Simon, K.P., 1982, Astron. Astrophys. 108, 387.

Stellar wind in the Nucleus of IC 2149, Perinotto, M., Benvenuti, P., Cerruti-Sola, M., 1982, Astron. Astrophys. 108, 314.

On the search for transition zone lines in late A type stars, Crivellari, L., Praderie, F., 1982, Astron. Astrophys. 107, 75.

The ultraviolet spectrum of CH Cygni during the outburst started in 1977, Hack, M., Selvelli, P.L., 1982, Astron. Astrophys. 107, 200.

Variability and mass loss in the extreme supergiant Sco, Burki, G., Heck, A., Bianchi, L., Cassatella, A., 1982, *Astron. Astrophys.* 107, 205.

IUE data reduction. The parameterization of the notion of the IUE reseaux grids and special formats as a function of time and temperature, Thompson, R.W., Turnrose, B. E., Bohlin, R.C., 1982, *Astron. Astrophys.* 107, 11.

Mg II h and k line observations delta Scuti variables, Fracassini, M., Pasinetti, L.E., 1982, *Astron. Astrophys.* 107, 326.

Infrared Photometry of Southern Be Stars, Dachs, J., Wamsteker, W. 1982, *Astron. Astrophys.* 107, 240 (1)

Detection of further Red Giants with "Hybrid" atmospheres and a possible correlation with double circumstellar Mg II and Ca II lines, Reimers, D., *Astron. Astrophys.* 107, 292.

The pulsation of the outer layers of the Beta Cephei-type variable BW Vul, Burger, M, de Jager, C., van der Oord, G.H.J., Sato, N., 1982, *Astron. Astrophys.* 107, 320.

On the ionization and velocity structure of expanding circumstellar envelopes, Drechsel, H., Rahe, J., 1982, *Astron. Astrophys.* 106, 70.

The variable shell star HR 5999 VI. Strong chromospheric and transition region emission lines in the Ultraviolet Spectrum of a Herbig Ae star, Tjin A Djie, H.R.E., The, P.S., Hack, M., Selvelli, P.L., 1982, *Astron. Astrophys.* 106, 98.

The absolute magnitudes of G5-M3 stars near the Giant branch, Egret, D., Keenan, P.C., Heck, A., 1982, *Astron. Astrophys.* 106, 115. (1)

Anomalous motions of HI clouds, Shaver, P.A., Radhakrishnan, V., Anantharamaiah, K.R., Retallack, D.S., Wamsteker, W., Danks, A.C., 1982, *Astron. Astrophys.* 106, 105. (1)

Hot stars in the bulge of M31: Upper limit to the star formation rate, Deharveng, J.M., Joubert, M., Monnet, G., Donas, J., 1982, *Astron. Astrophys.* 106, 16.

A study of ultraviolet spectroscopic and light variations in the X-ray binaries LMC X-4 and SMC S-1, van der Kilis, M., Hammerschlag-Hensberge, G., Bonnet-Bidaud, J.M., Ilovaisky, S.A., Mouchet, M., Glencross, W.M., Willis, A.J., van Paradijs, J.A., Zuiderwijk, E.J., Chevalier, C., 1982, *Astron. Astrophys.* 106, 339.

LB 3459 - An O type subdwarf eclipsing binary system. Non-LTE analysis of the primary, Kudritzki, R.P., Simon, K.P., Lynas-Gray, A.E., Kilkenny, D., Hill, P.W., 1982, *Astron. Astrophys.* 106, 254.

An alternative procedure for extracting IUE low resolution spectra, Crivellari, L., Morossi, C., 1982, *Astron. Astrophys.* 106, 332.

IUE ultraviolet spectrophotometry of 15 galactic Wolf-Rayet stars, Nussbaumer, H., Schmutz, W., Smith, L.J., Willis, A.J., 1982, *Astron. Astrophys. Suppl. Ser.* 47, 257.

The spectra of late-type dwarfs and sub-dwarfs in the near ultraviolet. I. Line identifications, *Astron. Astrophys. Suppl. Ser.* 47, 295.

The O-type subdwarf ROB 162 in the Globular Cluster NGC 6397, Caloi, V., Castellani, V., Panagia, N., 1982, *Astron. Astrophys.* 107, 145.

On excitation through radiative pumping of the Fe II UV-mult. 191 1785-88A observed with IUE during the eclipse of 32 Cyg., Hempe, K., Reimers, D., 1982, *Astron. Astrophys.* 107, 36.

Mass loss rates in the Open Cluster IC 1805, Llorente de Andres, F., Burki, G., Ruiz del Arbol, J.A., 1982, *Astron. Astrophys.* 107, 43.

On the detection of abundance stratifications in Peculiar Stars through the curve of growth method, Alecian, G., 1982, *Astron. Astrophys.* 107, 61.

New evidence of strong UV radiation in TT Ari, Wargau, W., Drechsel, H., Rahe, J., Vogt, N., 1982, *Astron. Astrophys.* 110, 281.

On the structure of the outer Layers of Cool Carbon stars, Querci, F., Querci, M., Wing, R.F., Cassatella, A., Heck, A., 1982, *Astron. Astrophys.* 111, 120.

The graphite rich Cepheus OB 3 association, Barsella, B., Panagia, N., Perinotto, M., 1982, *Astron. Astrophys.* 111, 130.

UV radiation from the young Sun and oxygen and ozone levels in the prebiological palaeo atmosphere, Canuto, V.M., Levine, J.S., Augustsson, T.R., Imhoff, C.L., 1982, *Nature* 296, 816.

IUE observations of variability and difference in the UV spectra of double quasar 0957 + 561 A,B, Gondhalekar, P.M., Wilson, R., 1982, *Nature* 296, 415.

The nearby interstellar medium, Frish, P.C., 1982, Nature 299, 377.

International Directory of Amateur, Heck, A., Manfroid, J., 1981, Astronomical Societies 1982, 312 p. (1)

The spectrum of HD 51585 in the Blue and in the Ultraviolet, in "Be Stars", L. Houziaux, L., Andriolat, Y., Nandy, K., Heck, A., 1982, Eds. M. Jaschek & H.G. Roth, D. Reidel & Co, Dordrecht, p. 427.

IUE observation statistics, in UV stellar classification, Heck, A., 1982, SP-182, p. 55.

IUE Data Distribution, in "Automated Data Retrieval in Astronomy", Heck, A., Eds. C. Jaschek & W. Heintz, D. Reidel Publ. Co, Dordrecht, p.29.

Carbon Abundance in the WC 10 star CPD -56 8032, in "Wolf-Rayet Stars: Observations, Physics and Evolution", Houziaux, L., Heck, A., 1982, Eds. C.W.H. de Loore & A.J. Willis, D. Reidel Publ. Co, Dordrecht, p. 139.

August 1981 Crisis of V348 Sgr, Heck, A., Houziaux, L., Manfroid, J., 1982, Comm. 27 IAU Inf. Bull. Stars 2184. (1)

Broad Band Linear Polarization and Magnetic Intensification in rotating magnetic stars, Landi degl' Innocenti, M., Landi degl' Innocenti, E., Calamai, G., Patriarchi, P., 1981, Ap. J., 249, 228. (1)

UV radiation from central stars of Planetary Nebulae, Cerruti-Sola, M., Cacciari, C., Patriarchi, P., Perinotto, M., 1982, Proceedings of IAU Symposium No. 103 on Planetary Nebulae (in press) ESA.

The papers indicated with (1) are publications by the IUE Observatory Staff not associated with results obtained through observations with the International Ultraviolet Explorer Sattelite.

THIRD EUROPEAN IUE CONFERENCE

Under the auspices of the European Space Agency and the Instituto de Optica (Daza de Valdez) the Third European IUE Conference was held on 10-13 May 1982 in Madrid. The Conference was attended by 166 participants from no less than 13 countries. The proceedings of the conference have already appeared in press, (due to extreme efficiency of the ESTEC publication department). Below we give the table of contents of the proceedings. The proceedings have been edited by E. Rolfe, A. Heck and B. Battrick as an ESA special publication (ESA-SP-176). Copies (175 F.F.) can be obtained from:

Distribution Office
ESA Scientific and
Technical Publication Branch
ESTEC
2200 AG Noordwijk
HOLLAND

TABLE OF CONTENTS ESA SP-176
(Third European IUE Conference)

INVITED PAPERS

The structure, energy balance and winds of cool stars.
J. Linsky

Stellar evolution after IUE: 1. Massive stars during core
hydrogen burning and massive close binaries.
C. de Loore & A. Maeder

Stellar evolution after IUE: 2. A renewal for massive
stars and WR stars.
A. Maeder & C. de Loore

Ultraviolet properties of supernovae.
N. Panagia

Interstellar gas studies with IUE.
M. Pettini

Review of galactic ultraviolet astronomy.
C. de Jager

IUE observations of giant planets, satellites and
asteroids.
T. Encrenaz

Stellar populations in normal galaxies.
M. Capaccioli

Active galaxies observed by IUE.
M.V. Penston

Extragalactic ultraviolet astronomy and cosmology.
M.S. Longair

CONTRIBUTED PAPERSSession 1: COOL STARS

An analysis of the ultraviolet spectrum of T Tauri.
C. Jordan, M.C. de Ferraz & A. Brown

T Tauri stars: Not one but two transition regions.
C. Bertout

Far UV line widths in RU Lupi.
M.V. Penston & M.T.V.T. Lago

On the MgII and FeII resonance lines in Herbig Ae Stars:
Preliminary analysis. A. Talavera, C. Catala, L.
Crivellari, J. Czarny,

Contribution to the study of the dust envelope of AB
Aurigae.
C. Catala

The variable shell star HR 5999 VII. The extended
atmosphere of a Herbig Ae star: Chromospheric features.
H.R.E. Tjin A Djie & P.S. The

Ultraviolet resonance line emissions observed by IUE.
C. Blanco, L. Bruca, S. Catalano & E. Marilli

Chromospheric MgII emission in A5 to K5 main sequence stars
from high resolution IUE spectra (abstract only).
C. Blanco et al.

Rotational modulation of chromospheric features in late-
type stars.
P.B. Byrne, C.J. Butler, A.D. Andrews, J.L. Linsky, T.
Simon, N. Marstadt, M. Rodono, C. Blanco, S. Catalano,
E. Marilli

IUE Observations of Classical Cepheids
W. Eichendorf, B. Reipurth, B. Caccin, G. Russo, C.
Sollazzo

Search for Ti II 5 multiplet emissions in selected Delta
Scuti variables.
F. Castelli, M. Fracassini & L.E. Pasinetti

FeII absorption lines in the IUE high-resolution spectra of
F supergiants and shell stars.
D.P. Gilra

Outer atmospheric properties of Beta Draconis (G2 Ib-II).
A. Brown, C. Jordan, T.R. Ayres, J.L. Linsky & R.E.
Stencel

A search for MgII h and k emission core variability in six main sequence stars.

J.E. Beckman, M.L. Franco, P. Molaro, G. Vladilo, L. Crivellari

The transition region structure of 'solar-like' stars.

M.J. Fernandez-Figueroa, E. de Castro & M. Rego

High resolution EUV spectroscopy of 56 Pegasi (KOIIP + wd).

C. Jordan, A. Brown, T.R. Ayres, J. Linsky & R.E. Stencel

Variability of cool stars at optical and ultraviolet wavelengths II - The binary (?) flare star AU Mic.

J.L. Linsky, P.L. Bornmann, M. Rodono, V. Pazzani, A.D. Andrews, C.J. Butler & P.B. Byrne

Stellar activity in the short period subgroup of the RS CVn systems.

E. Budding & A. Gimenez

Session 2: CATAclysmic Variables X-RAY SOURCES

Ultraviolet observations of nova Aquila 1982.

M.A.J. Snijders, M.J. Seaton & J.C. Blades

Simultaneous UV and optical observations of dwarf novae through outburst.

B.J.M. Hassall, J.E. Pringle, R.A. Wade & J.A.J. Whelan

The peculiar energy distribution of the old-nova GK Per (1901).

A. Bianchini & F. Sabbadin

The orbital variations of the UV spectrum of the old nova HR Del.

Y. Andrillat, M. Friedjung & P. Puget

The spectrum of the symbiotic star CH Cyg in December 1981.

M. Hack, M. Persi & P.L. Selvelli

Short-time spectral variations of the old nova RR Pi.

P.L. Selvelli

The spectrum of the old nova V 603 Aql between 2000 and 3200 Å.

P.L. Selvelli & A. Cassatella

A review of the ultraviolet results about symbiotic stars.

Friedjung & R. Viotti

Line shapes from the symbiotic star V 1016 Cyg.

H. Nussbaumer

A comparative study of IUE spectra of cataclysmic variables (abstract only).

C. la Dous

Strong UV excess radiation in cataclysmic variables.

W. Wargau, H. Drechsel & J. Rahe

Phase-dependent UV spectra of UX UMa.

A.R. King

Far UV observations of MV Lyrae in two different states.

L. Chiappetti, L. Maraschi, E.G. Tanzi & A. Treves

UV observations of V348 Sgr.

A. Heck, L. Houziaux, A. Cassatella, S. di Serego Alighieri & F. Macchetto

The UV variability of T Cr B.

A. Cassatella, P. Patriarchi, P.L. Selvelli, L. Bianchi, C. Cacciari, A. Heck, M. Perryman & W. Wamsteker

Ultraviolet, optical and infrared observations of HDE 245770/A 0535+26.

F. Giovannelli, C. de Loore, C. Bartolini, M. Burger, M. Ferrari Toniolo, A. Giangrande, A. Guarnieri, P. Persi, A. Piccioni & E.L. van Dessel

The ultraviolet spectra of newly discovered hard X-ray cataclysmic variables.

J.M. Bonnet Bidaud, M. Mouchet & Ch. Motch

Ultraviolet observations of V1341 = Cyg X2 (abstract only).

L. Chiappetti et al.

Ultraviolet observations of X-ray bursters.

G. Hammerschlag-Hensberge, J. van Paradijs & J.E. McClintock

On the UV variability of LSI + 61. 303 (=GT 0236) (abstract only).

E.G. Tanzi, G.F. Bignami, P.A. Caraveo, L. Maraschi, F. Sormani, A. Treves et al.

IUE high resolution observations of hot stars emitting coronal X-rays.

L. Bianchi

UV photometric and line-width variability of LMC X-4.

M. van der Klis, G. Hammerschlag-Hensberge, J.M. Bonnet-Bidaud, C. Chevalier, S.A. Ilovaisky, M. Mouchet, W.M. Glencross, A.J. Willis, J.A. van Paradijs, E.J. Zuiderwijk

The interacting binary KX And.
 F. Paterson-Beeckmans, A.M. Hubert-Delplace, H. Hubert &
 D. Ballereau

Session 3 : HOT STARS & BINARIES

Does the WC6 star HD76536 have a compact companion ?
 G.E. Bromage, W.M. Burton, K.A. van der Hucht, F.
 Macchetto & C.C. Wu

Mass loss from extreme helium stars.
 U. Heber, W.R. Hamann & D. Schoenberner

SK-67/111 and R 50, two Magellanic cloud emission line
 stars.
 F.J. Zickgraf, B. Wolf, R. Viotti, O. Stahl, O.
 Ricciardi, G. Muratorio, M. Friedjung & A. Cassatella

H-R diagram for early type Magellanic cloud members.
 K. Nandy, D.M. Morgan, G.I. Thompson, A. Willis, R.
 Wilson & L. Houziaux

A study of line profile variability in O-stars.
 R.G. Costero, M.L. Franco, E. Kontizas, M. Kontizas &
 R. Stalio

Empirical atmospheric velocity patterns from combined IUE
 and visual observation: The Be stars.
 V. Doazan & R.N. Thomas

Behaviour of the energy distribution of 59 Cyg in the far-
 ultraviolet and in the visible.
 L. Divan & J. Zorec

Envelope structure of the cyclic V/R variable shell stars
 (abstract only).
 A.M. Hubert-Delplace et al.

Non-LTE analysis of the SdO-star Feige 110.
 U. Hebert, W.R. Hamann, K. Hunger, R.P. Kudritzki, K.P.
 Simon & R.H. Mendez

Ultraviolet spectroscopy and effective temperature
 variations in the extreme helium star HD + 13 3224.
 A.E. Lynas-Gray, P.W. Hill & D. Schoenberner

Analysis of Feige 66, another extremely silicon-deficient
 OB subdwarf.
 B. Baschek, P. Hoflich & M. Scholz

The metallicity of the extreme helium star BD + 10 2179
 U. Heber

Radiative transfer calculations for the C IV 155 nm resonance lines in planetary nebulae.

J. Koppen & R. Wehrse

The planetary nebula NGC 6572.

M. Grewing, G. Kramer, P. Diets, P.R. Preassner

The UV stellar classification programme.

A. Heck, P. Benvenuti, L. Bianchi, J.C. Blades, C. Cacciari, A. Cassatella, A. Cucchiaro, D. Egret, C. Jashek, M. Jashek, K. Nandy, P. Patriarchi, W. Wamsteker, C.C. Wu

CV Serpentis: still eclipsing.

I.D. Howarth, A.J. Willis & D.J. Stickland

A study of CQ Cephei - far UV to infrared.

D.J. Stickland, W.M. Burton, G. Bromage, A.J. Willis, I.O. Howarth, E. Budding & R.F. Jameson

UV resonance line formation in Zeta Aur/UV Cep systems.

K. Hempe & D. Reimers

Evolution of the subdwarf-O eclipsing binary LB 3459.

R.P. Kudritzki, K.P. Simon, A.E. Lynas-Gray, D. Kilkenny & P.W. Hill

New observations of the interacting binary SV Cen.

H. Drechsel, W. Wargau & J. Rahe

The IUE survey of W UMa-type binaries.

S.M. Rucinski & O. Vilhu

Mass-loss rate from IUE observations of Zeta Aur systems.

A. Che, K. Hempe & V. Reimers

System parameters and mass-loss of Sge.

D. Reimers & K.P. Schroder

Analysis of UV spectra of Beta Lyrae.

H. Cugier

Session 4 : THE INTERSTELLAR MEDIUM

Analysis of extinction curves towards the SCO OBI association.

S. Aiello, B. Barsella & A. Bonetti

Anomalous extinction in the Cepheus OB 3 association.

B. Barsella, N. Panagia & M. Perinotto

- Dust properties in stellar groups.
P. Patriarchi, M. Perinotto & B. Barsella
- Interstellar extinction in anomalous regions.
J.C. Blades, L.A. Jacobs, D. McNally, W.B. Somerville & D.C.B. Whittet
- Ultraviolet interstellar extinction in the SMC from IUE stellar observations (abstract only).
M. Prevot et al.
- Interstellar lines in high resolution IUE spectra: Paper I Groningen Data Reduction package and technical results.
D.P. Gilra, T.H. Pwa, E.M. Arnal & J. de Vries
- Interstellar lines in high resolution IUE spectra: Paper II Highlights of preliminary astronomical results.
D.P. Gilra, T.H. Pwa & E.M. Arnal
- Studies of interstellar CO.
W.B. Somerville, L.A. Jacobs, D. McNally, D.C.B. Whittet & J.C. Blades
- High velocity gas components associated with supergiant stars and interstellar gas.
B. Bates, W. Brown-Kerr & D.L. Giaretta
- Depletion of interstellar zinc.
A.W. Harris, G.E. Bromage & J.C. Blades
- Element depletions in interstellar gas.
s A.P. Phillips, P.M. Gondhalekar & M. Pettini
- The Monoceros Loop: A supernova remnant interacting with the Rosette Nebula ?
A. Vidal-Madjar, C. Laurent, M. Pettini, J.A. Paul & M. Oliver
- The violent interstellar medium associated with the Carina Nebula.
C. Laurent, J.A. Paul & M. Pettini
- Interstellar gas in the direction of the large Magellanic Cloud.
D. Maslen, A.J. Willis, R. Wilson, K. Nandy & J.C. Blades
- Highly ionized gas in the galactic halo.
K.A. West & M. Pettini
- Distribution of gas in the halo of the galaxy.
J.C. Blades, L.L. Cowie, D.C. Morton, D.G. York & C.C. Wu
- Abundances in the Magellanic stream (abstract only).
M.V. Penston et al.

Session 6 : THE SOLAR SYSTEM

M.C. Festou, P.D. Feldman, M.A. Weaver & H.U. Keller

Are comets made of H₂O-ice ?

M.K. Wallis

Ammonia in the Jovian stratosphere: A comparison of photochemical calculations with IUE observations.

K.H. Fricke, U. von Zahn, M. Combes & Th. Encrenaz

Observations of the Lyman-Alpha albedo of Uranus.

S. K.H. Fricke & J.D. Darius

Session 6 : FUTURE UV EXPERIMENTS

Current NASA studies for a Far-Ultraviolet Spectrographic Explorer (FUSE).

J. Linsky et al.

Magellan - Far and extreme ultraviolet spectrographic observatory.

S. di Serego Alighieri

Exotic stellar objects: Research for the proposed satellite Magellan.

M. Hack

The interest of observing main sequence objects with Magellan.

F. Praderie

Observations in the solar system with the proposed earth-orbiting observatory Magellan.

R. Prange

Session 7 : EXTRAGALACTIC OBJECTS

UV energy distribution in elliptical galaxies.

F. Bertola, M. Capaccioli & G. Longo

Optical and ultraviolet spectrophotometry of globular clusters in the Magellanic clouds.

C. Cacciari, F. Fusi-Pecci, C. Zavaroni, K.C. Freeman, A. Cassatella, P. Benvenuti, A. Heck, P. Patrianichi, W. Wamsteker

UV observations of the young blue globular clusters in the LMC (abstract only).

A. Cassatella & E.H. Geyer

Optical and ultraviolet observations of the X-ray globular cluster Bo158 in M31.

C. Cacciari, A. Cassatella, L. Bianchi, F. Fusi-Pecci & R.G. Kron

Coordinated observations of Seyfert I galaxies.

W. Wamsteker, P. Benvenuti, C. Cacciari, A. Cassatella,
L. Bianchi, P. Patriarchi, J.C. Blades & A.C. Danks

Results from the NGC 4151 ultraviolet laboratory.

G.E. Bromage, A. Boksenberg, J. Clavel, A. Elvius, M.V.
Penston, & G.C. Perola, M. Pettini, M.A.J. Snijders,
E.G. Tanzi, M. Tarenghi, M.H. Ulrich

Monitoring the UV spectrum of the Seyfert Galaxy NGC 4593
II. Short term variability.

J. Clavel

NGC 7469, a Seyfert galaxy observed with IUE.

A. Elvius, B.A.M. Westin & J. Lind

Line profiles and continuum radiation in Seyfert galaxies.

C. Boisson & M.H. Ulrich

Secondary ultraviolet sources in the Seyfert-2 galaxy NGC
106B.

M.A.J. Snijders, S.A. Briggs & A. Boksenberg

IUE observations of NGC 3783.

P. Barr

Markarian 108. A tidally-torn off or turned on galaxy ?

P. Benvenuti, C. Casini & J. Heidmann

Ly alpha absorption at $CZ = 8200 \text{ km s}^{-1}$ in NGC 1275.

S.A. Briggs, M.A.J. Snijders & A. Boksenberg

The ultraviolet spectrum of the high-redshift BL Lac object
0215-015.

J.C. Blades, M. Pettini, R.W. Hunstead, H.S. Murdoch

Multifrequency observations of the OVV quasar 1156+295.

A.E. Glassgold, J.N. Bregman & P.J. Huggins

UV observations of X-ray emitting QSOs and BL Lac objects.

L. Chiappetti, L. Maraschi, E.G. Tanzi & A. Treves

Simultaneous multifrequency observations of BL Lac objects
and violently variable quasars.

J.N. Bregman, A.E. Glassgold & P.J. Huggins

Cosmology from IUE observations of quasars ? (abstract
only).

C.M. Gaskell

The formation of the broad emission line regions in QSOs.

J.E. Dyson & J.J. Perry

DATA PROCESSING

The IUE spectra of ET And: Their reduction and variation.
M. Barylak

LATE PAPER

Stellar winds.
C. de Loore

VILSPA IMAGES FOR RELEASE TO SCIENTIFIC COMMUNITY

1982 May 1st (despatched 1981 October)

Camera 1 LWPCamera 2 LWRCamera 3 SWP

1357	11645	11722	11805	15136	15207	15256
1358	11646	11723	11811	15137	15208	15265
1359	11652	11728	11817	15138	15209	15270
1360	11653	11732	11818	15139	15210	17275
1361	11662	11733	11819	15140	15214	15276
1363	11663	11734	11820	15147	15215	17277
1364	11664	11735	11827	15148	15216	15278
1365	11665	11736	11830	15149	15217	15289
	11672	11737	11831	15155	15218	15295
	11673	11744	11832	15156	15219	15296
	11674	11745	11849	15157	15220	15297
	11683	11753	11858	15165	15226	15298
	11684	11754	11859	15166	15227	15299
	11685	11755		15173	15228	15300
	11692	11769		15174	15229	15306
	11693	11770		15175	15230	15307
	11694	11778		15176	14237	15308
	11695	11779		15184	15238	15309
	11702	11780		15185	15239	15310
	11703	11781		15186	15244	15313
	11704	11784		15187	15250	15322
	11705	11785		15188	15251	15329
	11718	11789		15199	15252	15331
	11719	11790		15200	15253	15335
	11720	11791		15201	15254	15343
	11721	11804		15206	15255	15346

VILSPA IMAGES FOR RELEASE TO SCIENTIFIC COMMUNITY

1982 June 1st (despatched 1981 November)

<u>Camera 1 LWP</u>	<u>Camera 2 LWR</u>		<u>Camera 3 SWP</u>		
1369	11870	11965	15352	15467	15563
1370	11880	11966	15358	15468	15590
1371	11890	11967	15364	15469	15591
1373	11899	11968	15365	15472	15592
1374	11900	11969	15371	15484	
1387	11901	11976	15372	15485	
	11902	11977	15373	15486	
	11903	11984	15374	15487	
	11904	11992	15375	15488	
	11905	12002	15376	15489	
	11906	12003	15377	15498	
	11907	12004	15378	15499	
	11915	12005	15379	15530	
	11916	12006	15384	15531	
	11917	12007	15385	15532	
	11922	12017	15386	15533	
	11923	12018	15411	15534	
	11924	12019	15412	15539	
	11930	12020	15419	15540	
	11934	12021	15420	15541	
	11935	12022	15421	15542	
	11941	12030	15445	15543	
	11942	12031	15446	15544	
	11943	12032	15453	15549	
	11944	12033	15454	15550	
	11945	12043	15455	15551	
	11946	12050	15464	15552	
	11951	12057	15465	15558	
	11952	12058	15466	15562	

VILSPA IMAGES FOR RELEASE TO SCIENTIFIC COMMUNITY

1982 July 1st (despatched 1981 December)

<u>Camera 1 LWP</u>	<u>Camera 2 LWR</u>	<u>Camera 3 SWP</u>			
1396	12060	12143	15604	15710	15855
1397	12061	12144	15605	15711	15856
1398	12062	12151	15606	15712	15871
1399	12071	12153	15620	15713	15872
1403	12072	12154	15632	15718	15873
1408	12073	12164	15633	15734	15874
1409	12074	12165	15634	15735	15883
1410	12075	12166	15635	15736	15888
1411	12076	12167	15636	15737	15889
1412	12090	12191	15637	15738	15890
1413	12106	12192	15638	15739	15891
1414	12114	12193	15648	15747	15894
1415	12124	12208	15657	15761	15895
1416	12125	12209	15673	15762	
	12126	12210	15690	15763	
	12127	12211	15691	15792	
	12132	12222	15698	15793	
	12133	12225	15699	15794	
	12134	12226	15700	15795	
	12139	12227	15701	15822	
	12140	12231	15702	15832	
	12141	12232	15703	15833	
	12142		15709	15834	

VILSPA IMAGES FOR RELEASE TO SCIENTIFIC COMMUNITY

1982 August 1st (despatched 1982 January)

<u>Camera 1 LWP</u>		<u>Camera 2 LWR</u>			<u>Camera 3 SWP</u>		
1417	1454	12233	12316	12443	15902	15988	16129
1418	1455	12234	12317	12444	15903	15989	16130
1419	1456	12236	12318	12445	15907	15996	16131
1420	1457	12240	12325	12446	15908	15997	16132
1421	1458	12251	12326	12447	15915	15998	16133
1422	1459	12252	12327	12457	15916	15999	16134
1423	1460	12253	12328	12458	15917	16000	16135
1424	1461	12261	12340	12463	15918	16001	16136
1425	1462	12262	12345	12464	15926	16013	16157
1426	1463	12263	12346	12465	15927	16018	16158
1436	1464	12269	12347	12466	15928	16029	16159
1437	1465	12270	12348	12474	15938	16030	16160
1438	1466	12271	12349	12482	15939	16031	16161
1439	1467	12281	12359		15940	16032	16162
1440	1468	12282	12366		15941	16034	16163
1441	1469	12283	12378		15942	16035	16164
1442	1470	12284	12395		15950	16049	16165
1443	1471	12287	12407		15951	16050	16166
1444	1472	12288	12408		15952	16051	16167
1445	1473	12289	12413		15965	16052	16168
1446	1474	12293	12419		15966	16068	16197
1447	1475	12294	12420		15967	16075	16198
1448	1476	12295	12430		15968	16076	16199
1449	1477	12306	12433		15983	16103	16200
1450		12307	12439		15984	16104	16201
1451		12313	12440		15985	16119	16210
1452		12314	12441		15986	16127	16211
1453		12315	12442		15987	16128	

VILSPA IMAGES FOR RELEASE TO SCIENTIFIC COMMUNITY

1982 September 1st (despatched 1982 February)

<u>Camera 1 LWP</u>			<u>Camera 2 LWR</u>		<u>Camera 3 SWP</u>	
1488	12489	12554	12628	16228	16306	16411
1489	12490	12555	12629	16229	16311	16415
1490	12491	12556	12639	16230	16317	16416
1491	12492	12557	12640	16231	16318	16422
1492	12493	12558	12649	16232	16319	16423
1493	12494	12559	12650	16233	16320	16430
	12495	12560	12651	16242	16327	
	12503	12564	12652	16243	16328	
	12506	12565	12662	16253	16329	
	12507	12566	12665	16254	16330	
	12515	12567	12675	16263	16346	
	12519	12578	12676	16264	16347	
	12523	12579	12677	16265	16348	
	12528	12580	12681	16274	16349	
	12529	12581		16278	16363	
	12530	12588		16284	16374	
	12531	12595		16285	16375	
	12532	12596		16286	16376	
	12534	12597		16287	16377	
	12542	12598		16288	16373	
	12543	12599		16289	16379	
	12544	12612		16290	16390	
	12545	12618		16291	16398	
	12546	12619		16295	16399	
	12547	12620		16303	16400	
	12552	12626		16304	16401	
	12553	12627		16305	16410	

VILSPA IMAGES FOR RELEASE TO SCIENTIFIC COMMUNITY

1982 October 1st (despatched 1982 March)

<u>Camera 1 LWP</u>		<u>Camera 2 LWR</u>			<u>Camera 3 SWP</u>	
1497	12695	12795	12834	16454	16527	16603
1498	12696	12796	12835	16455	16528	16611
1499	12697	12797	12842	16456	16529	16612
1500	12703	12798	12843	16457	16530	16613
1501	12704	12799	12844	16459	16540	16620
1502	12705	12800	12845	16460	16541	16627
1503	12710	12801	12850	16467	16542	16628
	12711	12802	12851	16476	16543	16629
	12724	12805	12852	16478	16544	16644
	12728	12806	12863	16485	16552	16645
	12729	12807	12864	16486	16553	16649
	12758	12808	12865	16487	16554	16650
	12764	12809	12866	16488	16555	16651
	12765	12810	12879	16493	16561	16659
	12774	12811	12888	16494	16562	16664
	12775	12812	12903	16495	16563	16665
	12780	12813	12904	16504	16564	16666
	12782	12814	12914	16505	16573	16667
	12783	12815	12915	16516	16574	16669
	12784	12816	12916	16517	16575	16670
	12785	12817	12917	16518	16580	
	12786	12826	12918	16519	16581	
	12794	12833	12919	16526	16590	
			12920			

VILSPA IMAGES FOR RELEASE TO SCIENTIFIC COMMUNITY

1982 November 1st (despatched 1982 April)

<u>Camera 1 LWP</u>	<u>Camera 2 LWR</u>	<u>Camera 3 SWP</u>		
1510	12925	13013	16675	16740
1511	12926	13014	16676	16741
1512	12927	13020	16677	16747
1513	12928	13025	16678	16749
1514	12943	13030	16683	16752
1523	12950	13036	16684	16753
1524	12951	13049	16686	16754
1525	12952	13063	16687	16760
1526	12963	13092	16694	16761
1527	12964	13100	16695	16782
1528	12965	13101	16696	16811
1529	12972	13102	16697	16816
1530	12973		16698	16824
1531	12981		16699	16829
1532	12990		16707	16835
1533	12998		16708	16842
	12999		16718	16846
	13006		16719	16854
	13007		16729	16855
	13012		16730	

VILSPA IMAGES FOR RELEASE TO SCIENTIFIC COMMUNITY

1982 December 1st (despatched 1982 May)

<u>Camera 1 LWP</u>	<u>Camera 2 LWR</u>	<u>Camera 3 SWP</u>
1534	13113	13279
1535	13123	13286
1536	13124	13291
1547	13134	13306
1548	13135	13307
1553	13147	13308
1554	13148	13326
	13159	13359
	13171	13360
	13184	
	13185	
	13186	
	13187 /	
	13213	
	13223	
	13234	
	13241	
	13249	
	13257	
	13258	
	13259	
	13260	
	13268	
	13269	
	13270	
		16863
		16864
		16865
		16866
		16867
		16868
		16869
		16870
		16871
		16872
		16879
		16882
		16886
		16888
		16890
		16899
		16909
		16910
		16911
		16912
		16913
		16914
		16915
		16925
		16926
		16927
		16935
		16936
		16937
		16945
		16956
		16957
		16958
		16971
		16972
		16976
		16987
		16988
		16989
		16990
		16999
		17008
		17009
		17018
		17019
		17029
		17030
		17033
		17034
		17035
		17036
		17037
		17038
		17039
		17040
		17053
		17067
		17068
		17069
		17075
		17076

VILSPA IMAGES FOR RELEASE TO SCIENTIFIC COMMUNITY

1983 January 1st (despatched 1982 June)

<u>Camera 1 LWP</u>	<u>Camera 2 LWR</u>	<u>Camera 3 SWP</u>		
1565	13370	13464	17085	17203
1566	13371	13465	17086	17211
1567	13379	13466	17087	17228
1568	13380	13470	17093	17238
1569	13390	13479	17094	17239
1570	13391	13480	17095	17249
1571	13392	13481	17096	17250
1572	13393	13482	17097	17257
1573	13400	13489	17104	17265
1574	13413	13497	17105	17266
1581	13414	13503	17127	17278
1582	13415	13504	17135	17284
1583	13424	13514	17136	17285
1584	13425	13515	17140	17286
	13432	13522	17141	17304
	13433	13523	17147	17313
	13447	13528	17168	
	13448	13533	17169	
	13449	13548	17170	
	13450	13549	17179	
	13461	13565	17180	
	13462	13569	17181	
	13463		17197	

INTERNATIONAL ULTRAVIOLET EXPLORER

ESA LOG OF IMAGES

01MAY82 - 30SEP82

SORTED BY STELLAR COORDINATES

PROGRAMME REFERENCE NUMBERS FOR THE PROGRAMME
IDENTIFICATION IN THIS LISTING CAN BE FOUND IN
I U E E S A NEWSLETTER NO. 13 (JUNE 1982),
PAGE 43.

CLASSIFICATION OF OBJECTS USED IN THE JOINT ESA/SRU LOG OF IUE OBSERVATIONS

00 SUN	50 R,N OR S TYPES
01 EARTH	51 LONG PERIOD VARIABLE STARS
02 MOON	52 IRREGULAR VARIABLES
03 PLANET	53 REGULAR VARIABLES
04 PLANETARY SATELLITE	54 DWARF NOVAE
05 MINOR PLANET	55 CLASSICAL NOVAE
06 COMET	56 SUPERNOVAE
07 INTERPLANETARY MEDIUM	57 SYMBIOTIC STARS
08	58 T TAURI
09	59 X-RAY
10 W C	60 SHELL STAR
11 W M	61 ETA CARINAE
12 MAIN SEQUENCE O	62 PULSAR
13 SUPERGIANT O	63 NOVA-LIKE
14 OE	64 STELLAR OBJECT NOT INCLUDED ABOVE
15 OF	65
16 SD O	66
17 WD O	67
18	68
19 UV-STRONG	69
20 B0-B2 V-IV	70 PLANETARY NEBULA + CENTRAL STAR
21 B3-B5 V-IV	71 PLANETARY NEBULA - CENTRAL STAR
22 B6-B9.5 V-IV	72 H II REGION
23 B0-B2 III-I	73 REFLECTION NEBULA
24 B3-B5 III-I	74 DARK CLOUD (ABSORPTION SPECTRUM)
25 B6-B9.5 III-I	75 SUPERNOVA REMNANT
26 BE	76 RING NEBULA (SHOCK IONISED)
27 BP	77
28 SDB	78
29 WDB	79
30 A0-A3 V-IV	80 SPIRAL GALAXY
31 A4-A9 V-IV	81 ELLIPTICAL GALAXY
32 A0-A3 III-I	82 IRREGULAR GALAXY
33 A4-A9 III-I	83 GLOBULAR CLUSTER
34 AE	84 SEYFERT GALAXY
35 AM	85 QUASAR
36 AP	86 RADIO GALAXY
37 WDA	87 BL LACERTAE OBJECT
38	88 EMISSION LINE GALAXY (NON-SEYFERT)
39 COMPOSITE	89
40 F0-F2	90 INTERGALACTIC MEDIUM
41 F3-F9	91
42 FP	92
43 LATE TYPE DEGENERATE STARS.	93
44 G (TO 1FEB79); GIV-VI (FROM 1FEB79)	94
45 G I-II (FROM 1FEB79)	95
46 K (TO 1FEB79); K IV-VI (FROM 1FEB79)	96
47 K I-III (FROM 1FEB79)	97
48 M (TO 1FEB79); M DWARFS (FM 1FEB79)	98 WAVELENGTH CALIBRATION (NASA LOG)
49 M I-III (FROM 1FEB79)	99 NULLS AND FLAT FIELDS (NASA LOG)

THE CLASSIFICATION IS SUPPLIED BY D STICKLAND FOR USE ONLY WITHIN THE PROJECT

EXPOSURE CLASSIFICATION CODES

SINCE 1 AUG 78 A TWO-DIGIT CODE HAS BEEN USED TO DESCRIBE EXPOSURE LEVELS. THIS CODE OCCUPIES THE FIRST TWO CHARACTER POSITIONS OF THE COMMENT FIELD.

DIGIT 1: EXPOSURE LEVEL OF CONTINUUM
DIGIT 2: EXPOSURE LEVEL OF EMISSION LINES

THE CLASSIFICATIONS BELOW APPLY TO BOTH:

- 0: NOT APPLICABLE
- 1: NO SPECTRUM VISIBLE
- 2: FAINT SPECTRUM; MAX DN < 20 ABOVE BACKGROUND
- 3: UNDEREXPOSED; MAX DN < 100 ABOVE BACKGROUND
- 4: WEAK; MAX DN BETWEEN 100 AND 150 ABOVE BACKGROUND
- 5: GOOD; NO SATURATION BUT MAX DN OVER 150 ABOVE BACKGROUND
- 6: A BIT STRONG; A FEW PIXELS SATURATED
- 7: SATURATED FOR LESS THAN HALF THE SPECTRUM
- 8: MOSTLY SATURATED BUT SOME PARTS USABLE
- 9: COMPLETELY SATURATED

ON 1 SEP 79 A FURTHER DIGIT WAS ADDED TO DESCRIBE THE LEVEL OF THE BACKGROUND. THE MEAN DN GIVEN BY A SUBSET HISTOGRAM OF WIDTH 2 PIXELS BETWEEN:

SWP 550,130 AND 685,310
AND LWR 160,195 AND 90,300

HAS BEEN CODED AS FOLLOWS: (LIMITS INCLUSIVE)

- 0 DN<20
- 1 21<DN<30
- 2 31<DN<40
- 3 41<DN<50
- 4 50<DN<60
- 5 60<DN<70
- 6 71<DN<80
- 7 80<DN<90
- 8 91<DN<100
- 9 DN>101
- X SATURATED

OBJECT	CL	MAG	RT	ASCN	DECL	DISP	APERT	START	LENGTH	PROG	COMMENT
			HR	MIN	SC	DEG	MIN	HR	MIN	SC	
0521-364	87	15.5	05	21	13	-36 30	L 2	05MAY82	00 39 25	260 00	EE168 307
0521-364	87	15.5	05	21	13	-36 26	L 3	01MAY82	00 44 21	226 00	EE168 232
NGC 1987	83	12.1	05	27	54	-70 47	L 2	25AUG82	18 38 43	425 00	GLOBC 309 4-MIN-HTR-MM-UP
NGC 2004	83	9.9	05	30	44	-07 19	L 2	02JUN82	22 33 15	043 00	EE176 501
NGC 2004	83	09.9	05	30	45	-07 19	H 1	11MAY82	00 54 52	393 00	EE174 305
NGC 2004	83	9.9	05	30	45	-07 19	H 3	07JUN82	22 36 39	430 00	EE176 304
IU ORI	58	09.2	05	32	08	-05 44	L 2	30AUG82	18 43 04	030 00	EC271 303 4-MIN-HTR-MM-UP, MN805
IU ORI	58	09.2	05	32	08	-05 44	L 3	30AUG82	19 16 27	150 00	EC271 302
HD 269696	16	11.2	05	32	08	-69 55	H 1	31AUG82	18 30 58	085 00	EI239 403
HD 269696	16	11.2	05	32	08	-69 55	L 1	31AUG82	22 32 52	002 00	EI239 502
HD 269696	16	11.2	05	32	08	-69 55	L 3	31AUG82	20 10 21	001 30	EI239 501 REF PT -34,-204
HD 269696	16	11.2	05	32	08	-69 55	L 3	31AUG82	20 03 11	001 15	EI239 401 REF PT 2,-212
HD 269696	16	11.2	05	32	08	-69 55	H 3	31AUG82	20 49 07	100 00	EI239 501
HD 269696	16	11.2	05	32	08	-69 55	H 3	31AUG82	22 59 44	100 00	EI239 502
HD 269696	16	11.2	05	32	08	-69 55	H 2	31AUG82	22 59 32	150 00	EA069 504 4-MIN-HTR-MM-UP, MN720
-5 1305	30	08.0	05	32	20	-05 36	H 2	14015	20 09 32	150 00	EA069
HD 36861	12	3.8	05	32	23	+09 54	H 3	17860	18 45 32	000 30	EI273 701
HD 36861	12	3.8	05	32	23	+09 54	H 3	17934	16 32 26	000 20	EA087 501
HD 36861	13	3.3	05	32	23	+09 54	H 3	17968	19 02 45	000 20	EA087 501
HD 36861	12	3.8	05	32	23	+09 54	H 3	18010	16 50 23	000 20	EI273 601
HD 36861	12	3.8	05	32	23	+09 54	H 3	18050	16 40 55	000 20	EI273 501
HD 36861	12	3.8	05	32	23	+09 54	H 3	18165	19 15 50	000 20	EI273 501
HD 36861	12	3.8	05	32	24	+09 54	H 3	17901	19 07 06	000 25	EI273 701
HD 36861	12	3.8	05	32	24	+09 54	H 3	18096	16 47 17	000 20	EI273 501
PI 2441	58	10.8	05	34	23	-14 27	L 2	14061	22 27 59	030 00	EC271 352 4-MIN-HTR-MM-UP
PI 2441	58	10.8	05	34	23	-14 27	L 3	17814	23 03 20	165 00	EC271 222
HD 37202	26	2.8	05	34	39	+21 07	H 2	14078	23 15 55	000 50	EA166 712
HD 37202	26	2.8	05	34	39	+21 07	H 3	17842	23 12 17	000 40	EA166 611
A0538-66	59	13.2	05	35	42	-06 54	L 2	13615	20 57 57	030 00	EM242 402
A0538-66	59	13.2	05	35	42	-06 54	L 3	17365	21 32 57	060 00	EM242 441
0538-66A	13	13.5	05	35	43	-06 54	L 3	17371	22 50 52	040 00	EM242 501 STAR A IN A0538 FIELD
0538-669	59	13.5	05	35	43	-06 54	L 3	18167	22 04 23	062 00	EI273 301 TWO STARS IN APERTURE
NGC 2100	83	09.6	05	42	23	-69 15	H 3	17575	18 51 09	359 00	VILSP 304
C AUSTIN	06	7.0	05	43	28	-21 04	L 2	13791	21 29 00	025 00	EST00 372 4-MIN-HTR-MM-UP
C AUSTIN	06	7.0	05	43	28	-21 04	L 2	13792	22 45 36	030 00	EST00 051 4-MIN-HTR-MM-UP
C AUSTIN	06	7.0	05	43	28	-21 04	L 3	17512	21 57 43	002 00	EST00 131
HD 39801	49	00.8	05	52	28	+07 24	H 3	17725	18 53 38	370 00	EC232 132
IC 2149	70	11.0	05	52	41	+46 36	L 2	14220	18 52 16	006 00	EA254 502 4-MIN-HTR, MN=823
HD 45166	10	10.0	06	23	36	+08 30	L 2	14102	20 00 23	001 50	EI273 502 4-MIN-HTR, MN=704
HD 45166	10	10.0	06	23	36	+08 30	L 3	17861	19 41 40	002 00	EI273 551
HD 45166	10	10.0	06	23	36	+08 30	L 3	17969	19 42 30	002 00	EI273 501
HD 45166	11	9.9	06	23	36	+08 30	L 3	18009	16 13 09	002 00	EI273 550
A 15	70	15.7	06	24	59	-25 21	L 3	16925	20 57 48	080 00	EA137 501
+34 1543	16	9.4	07	06	58	+34 30	H 3	17959	18 21 57	180 00	EA011 502
-44 3318	40	10.0	07	17	56	-44 30	L 2	14023	18 22 20	090 00	EA069 704 4-MIN-HTR-MM-UP, MN724
-44 3318	40	10.0	07	17	56	-44 30	L 2	14025	21 49 11	015 00	EA069 342 4-MIN-HTR-MM-UP
-44 3318	40	10.0	07	17	56	-44 30	L 3	17779	18 36 31	060 00	EA069 341
-44 3318	40	10.0	07	17	56	-44 30	L 3	17788	19 55 31	110 00	EA069 551
A 20	70	16.6	07	20	22	+01 51	L 3	16927	05 02 37	143 00	EA137 501

OBJECT	CL	MAG	RT	ASCN	DEC	PRG	APERT	DATE	START	LENGTH	PROG	COMMENT
			HR	MIN	SEC	DEG	IN	DATE	HR	MIN	SEC	
NGC 2392	71	10.4	07	26	13	+21 01	L 2	14221	20 03 49	060 00	EA254	5334-MIN-HTR,11ASEC WEST
NGC 2392	71	10.4	07	26	13	+21 01	L 3	16043	19 33 08	015 00	EA254	301 11ARCSEC WEST-STAR
0729+103	59	14.5	07	29	44	+10 05	L 2	14094	17 54 33	025 00	E1060	302 4-MIN-HTR
0729+103	59	14.5	07	29	44	+10 05	L 3	17953	17 00 02	050 00	E1060	301
HD 60753	21	06.7	07	32	08	+50 25	L 1	1629	01 28 36	000 06	PHCAL	501
-31 4800	16	10.5	07	34	35	+32 06	H 2	13594	22 55 05	080 00	EA008	404
+75 325	16	9.5	08	04	43	+75 07	L 1	1676	19 30 41	000 40	PHCAL	503
+75 325	16	9.5	08	04	43	+75 07	L 1	1675	19 34 56	000 20	PHCAL	403
+75 325	16	9.5	08	04	43	+75 07	L 1	1677	20 08 25	001 20	PHCAL	503 TRAIL,I=3,R=0.60
+75 325	16	09.5	08	04	43	+75 07	L 2	13186	05 08 02	036 00	PHCAL	501 4-MIN-HTR-M-UP
+75 325	16	09.5	08	04	43	+75 07	L 2	13157	07 12 43	001 20	PHCAL	501 TRAIL,R=0.25,1ITER
+75 325	16	9.5	08	04	43	+75 07	L 2	13466	05 44 16	001 12	PHCAL	402
+75 325	16	9.5	08	04	43	+75 07	L 2	13466	05 39 53	000 24	PHCAL	502
+75 325	16	9.5	08	04	43	+75 07	L 2	14233	16 54 17	000 48	PHCAL	502 MN=194
+75 325	16	9.5	08	04	43	+75 07	L 2	14233	16 50 15	000 24	PHCAL	502 MN=194
+75 325	16	9.5	08	04	43	+75 07	L 2	14234	17 30 39	001 14	PHCAL	402 MN=307,TR,I=3,R=0.61
+75 325	16	09.5	08	04	43	+75 07	L 3	16914	06 39 20	000 43	PHCAL	501 TRAIL,R=43.4,1ITER
+75 325	16	09.5	08	04	43	+75 07	L 3	16915	07 46 09	001 07	PHCAL	501 TRAIL,R=0.30,1ITER
+75 325	16	9.5	08	04	43	+75 07	L 3	18065	18 52 14	000 26	PHCAL	501
+75 325	16	9.5	08	04	43	+75 07	L 3	18065	18 48 08	000 14	PHCAL	501
+75 325	16	9.5	08	04	43	+75 07	L 3	18066	19 18 35	000 43	PHCAL	401 TRAIL,I=3,R=1.34
L532-81	37	12.0	08	39	34	-32 47	L 2	13549	02 22 04	045 00	EA144	602 MN=528
L532-81	37	12.0	08	39	34	-32 47	L 3	17286	00 37 01	090 00	EA144	501
A 31	70	15.5	03	51	36	+09 06	L 3	16925	03 22 54	040 00	EA137	101 WRONG STAR
IC 2448	70	12.5	09	06	33	+59 44	L 2	13759	09 10 29	195 00	EA165	345
IC 2448	70	12.5	09	06	33	+59 44	L 3	17473	21 06 15	180 00	EA165	372
IC 2448	70	12.5	09	06	33	+59 44	L 3	17474	03 29 28	010 00	EA165	451
+81 266	16	11.9	09	13	43	+81 56	L 3	17344	01 17 41	150 00	EA008	401
KS 292	16	11.3	09	18	20	+45 19	L 2	14101	16 47 09	002 00	EA035	502 4-MIN-HTR
KS 292	16	11.3	09	18	20	+45 19	L 3	17910	16 41 40	001 30	EA035	600
KS 292	16	11.3	09	18	20	+45 19	L 3	17911	17 15 49	125 00	EA035	502
NGC 2903	80	10.0	09	29	20	+21 43	L 2	13279	04 13 35	210 00	EM264	306 4-MIN-HTR-M-UP
NGC 2903	80	10.0	09	29	20	+21 43	L 3	16999	01 06 31	180 00	EM264	302
NGC 2903	80	12.0	09	29	20	+21 43	L 3	17085	00 45 58	195 00	EE207	312
HD 82901	51	7.0	09	30	59	+62 34	H 1	1609	20 35 08	017 00	EC275	032
HD 82901	51	09.0	09	30	59	+62 34	H 2	14103	20 55 32	060 00	E1273	132 4-MIN-HTR, MN=265
HD 82901	51	8.0	09	30	59	+62 34	L 2	14161	23 15 26	003 00	E1220	132 MN=371
NGC 2997	80	12.0	09	43	27	+39 58	L 2	13489	22 51 03	180 00	EE211	306 4-MIN-HTR-M-UP
NGC 2997	80	12.0	09	43	27	+39 58	L 3	17211	22 42 55	210 00	EE216	301
SA02740a	00	09.4	09	48	31	+55 54	L 1	1566	05 50 13	001 30	EE521	401
0957+561	85	17.5	09	57	57	+56 08	L 1	1565	23 37 15	323 00	EE521	233
+18 2307	46	9.7	09	58	56	+17 39	L 2	13479	22 55 11	025 00	EC048	233
+18 2307	46	9.7	09	58	56	+17 39	L 2	13480	02 29 11	025 00	EC048	233
+18 2307	46	9.7	09	58	56	+17 39	L 2	13481	03 42 33	040 00	EC048	343
+18 2307	46	9.7	09	58	56	+17 39	L 2	13482	05 00 16	040 00	EC048	333
+18 2307	46	9.7	09	58	56	+17 39	L 3	17197	23 24 30	251 00	EC048	122 SEE VILSPA L17
HD 8836a	51	7.0	10	04	46	+61 18	H 1	1610	21 35 40	060 00	EC275	032
HD 8836a	51	8.0	10	07	46	+61 18	L 2	14135	19 44 34	100 00	E1273	104 4-MIN-HTR

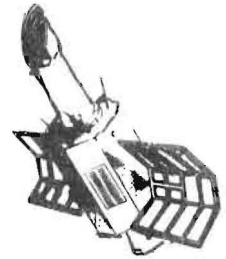
OBJECT	CL	MAG	RT ASCN			DEC			IMAGE	APERT		DATE	START			LENGTH		PRG	COMMENT	
			HR	MIN	SC	DEG	MIN	SEC		OB	LG		HR	MIN	SC	MIN	SC			
HD223047	45	05.0	23	43	33	+46	09	L	2	13837	S	0	02AUG82	00	43	57	003	00	EC201	502 MN#475
HD223047	45	05.0	23	43	33	+46	09	L	2	13837	L	0	02AUG82	00	37	42	003	00	EC201	702
HD223047	45	05.0	23	43	33	+46	09	L	3	17558	S	0	02AUG82	01	30	52	016	00	EC201	601
HD223047	45	05.0	23	43	33	+46	09	L	3	17558	L	0	02AUG82	01	06	12	020	00	EC201	801
SB 939	16	10.3	23	57	46	-39	41	L	2	14142	L	0	10SEP82	20	18	42	002	00	EA035	502 4-MIN-HTR
SB 939	16	10.3	23	57	46	-39	41	L	3	17912	L	0	10SEP82	20	49	40	003	00	EA035	500



THE EUROPEAN SPACE AGENCY

invites applications for

IUE RESIDENT ASTRONOMER



AT THE OBSERVATORY AT VILLAFRANCA, MADRID, SPAIN

Applications are invited for Resident Astronomer positions, available in 1982, at the IUE Observatory located near Madrid, Spain. The successful candidates will be expected to assist and advise visiting astronomers at the Observatory in their preparations and observations with IUE. In addition, each of the Resident Astronomers has responsibilities concerned with the scientific performance of the satellite or aspects of the running of the Observatory. They are expected to be post-doctoral astronomers who will undertake their own research programmes and participate also in the Observatory observing programme. Appointments will be for two years in the first instance. Salaries are good and commensurate with experience and the level of responsibility.

Applications or enquiries should be addressed to Dr. B. Fitton, Head Astronomy Division, ESA/ESTEC, P.O. Box 299, 2200 AG Noordwijk, The Netherlands.

ERRORS IN FOREGOING VILSPA LOG

Please inform us by post of all errors or omissions in the log reproduced in this issue. Detach this page, fold and staple it leaving the mailing address (verso) visible.

CAMERA & IMAGE	DISPERSION	APERTURE	TARGET	DATE OF OBSERVATION	WRONG FIELD CONTENTS	CORRECT INFORMATION

Dr. Chris Blades

UK Resident Astronomer

Villafranca Satellite Tracking Station

Apartado 54065

Madrid, Spain

QUESTIONNAIRE FOR NEWSLETTER CIRCULATION

- There is a misprint in my name/address on the present mailing label; the correct version appears below.
- Having become acquainted with the ESA IUE Newsletter through a colleague/library, I would like to be placed on the regular mailing list. My name and address, including the post code, are given below.
- Please delete my name and address (printed below) from the Newsletter distribution list.

NAME :

ADDRESS :

Now tear off this last page and return it to ESA, Paris, in the convenient posting format provided. Simply fold and staple leaving the mailing address (verso) visible.

Mrs. S. Babayan
European Space Agency
8-10 rue Mario-Nikits
75738 Paris Cedex 15
France